CSIRO PUBLISHING

RESEARCH ARTICLE
https://doi.org/10.1071/ES21014

JOURNAL OF SOUTHERN HEMISPHERE EARTH SYSTEMS SCIENCE

A catalogue of marine heatwave metrics and trends for the Australian region

Jules B. Kajtar[A,B,*], Neil J. Holbrook[A,B] and Vanessa Hernaman[C]

For full list of author affiliations and declarations see end of paper

***Correspondence to:**
Jules B. Kajtar
Institute for Marine and Antarctic Studies, University of Tasmania, Hobart, Tas., Australia
Email: jules.kajtar@utas.edu.au

ABSTRACT

Marine heatwaves around Australia, and globally, have been increasing in their frequency, intensity, and duration. This study reviews and catalogues marine heatwave metrics and trends around Australia since 1982, from near the beginning of the satellite sea-surface temperature observing period. The years in which the longest and strongest marine heatwaves around Australia occurred are also recorded. In addition, we analyse marine heatwaves in selected case study regions, and provide a short review of their associated impacts. These regions include: off the Western Australian coast, Torres Strait, Great Barrier Reef, Tasman Sea, and South Australian Basin. Finally, we provide a brief review of progress in understanding the potential predictability of sea surface temperature changes and marine heatwaves around Australia.

Keywords: Australian climate, case studies, extreme events, marine heatwaves, observations, potential predictability, sea surface temperature, trends.

Received: 3 June 2021
Accepted: 12 October 2021
Published: 14 December 2021

Cite this:
Kajtar JB *et al.* (2021)
Journal of Southern Hemisphere Earth Systems Science
71(3), 284–302. doi:10.1071/ES21014

1 Introduction

Marine heatwaves (MHWs) have been increasing in their frequency, intensity, and duration across most of the world's oceans (Oliver *et al.* 2018*a*; Laufkötter *et al.* 2020) and coastal regions (Marin *et al.* 2021) over the past century. These changes are largely due to anthropogenically-forced increases in air and ocean temperatures (Oliver *et al.* 2018*a*; Oliver 2019), with further increases expected under continued global warming (Frölicher *et al.* 2018; Oliver *et al.* 2019). Marine heatwaves can cause severe ecological impacts, such as coral bleaching (Hughes *et al.* 2017), mass mortality or redistribution of fish and invertebrates (Bond *et al.* 2015; Wernberg *et al.* 2016; Ugalde *et al.* 2018; Caputi *et al.* 2019; Smale *et al.* 2019), and loss of seagrass and kelp forests (Wernberg *et al.* 2013, 2016; Arias-Ortiz *et al.* 2018; Smale *et al.* 2019; Thomsen *et al.* 2019). Such environmental damage has human societal consequences, such as catch quota restrictions (Caputi *et al.* 2019), fishery closures (Cavole *et al.* 2016; Di Lorenzo and Mantua, 2016; Caputi *et al.* 2019), trade tensions among nations (Mills *et al.* 2013), food poisoning and shortages (Llewellyn 2010; Skinner *et al.* 2011), and cultural and food security impacts to indigenous peoples (Johnson *et al.* 2018, 2020).

Australia is home to a diverse, fragile, economically vital, and culturally significant marine environment. As the world's largest coral reef ecosystem, and a World Heritage site, the Great Barrier Reef (GBR) has extensive indigenous, social, historic, scientific, and natural value (GBRMPA 2014; Smith and Spillman 2019). It also supports 64 000 jobs, contributing A$6.4 billion per annum to the Australian economy (Smith and Spillman 2019). However, over the period 2015–2020, the GBR experienced three mass coral bleaching events, caused by MHWs (Bureau of Meteorology 2020). Immediate action is necessary to curb global warming, and to protect the future of the GBR (Hughes *et al.* 2017).

A number of other Australian marine regions have been identified as having significant value. McInnes *et al.* (2021) proposed five criteria for gauging such significance. These include socio-economic or traditional value, vulnerability to climate change, severity of projected impacts, potential for predictability, and potential for adaptation.

Under these criteria, the Western Australian coast, Tasman Sea, and Torres Strait were identified, along with the GBR (McInnes *et al.* 2021).

Under projected climate changes, MHWs around Australia are expected to increase in their severity and duration primarily due to mean temperature change, but changes in variability may also be important in some regions (Misra *et al.* 2021). It is because Australia's marine environment is diverse and valuable, but fragile to the potential damage from climate change, that a focused review of historical MHW metrics and trends around Australia is timely.

This study catalogues the Australian region MHW history over the satellite observational period during 1982–2020, for which the most accurate and homogeneous sea surface temperature (SST) data are available at daily resolution (described in Section 2). Broad MHW metrics and trends are presented in Section 3, with a closer examination of the most extreme events occurring in case study regions presented in Section 4.

Despite the clear and often devastating impacts of heatwaves on marine life (e.g. Smale *et al.* 2019), our knowledge of MHW predictability remains in its infancy. Nevertheless, research over the past several decades has culminated in increased process-based understanding of the mechanisms that cause MHWs around the world (Holbrook *et al.* 2019), providing us with a segue to now usefully consider their potential predictability, the development of operational prediction systems, and the implications of long-term projections (Holbrook *et al.* 2020*b*). Now, more than ever, there is a compelling need to understand the predictability of MHWs to help guide conservation, fisheries management, and aquaculture practices in a warming world (Holbrook *et al.* 2020*b*). A review on the progress of the potential predictability of SST and MHWs, with a focus on the Australian region, is presented in Section 5, followed by discussion and conclusions in Section 6.

2 Data and methods

MHWs around Australia have been analysed in this study from observational SST data, using the 0.25° gridded Daily Optimum Interpolation Sea Surface Temperature (DOISST), version 2.1, provided by the National Oceanic and Atmospheric Administration (NOAA; Huang *et al.* 2021*a*). The DOISST product represents a combination of observations from satellites, ships, buoys, and Argo floats mapped onto a regular global 0.25° grid. A spatially complete SST field is produced by interpolation to fill gaps (Reynolds *et al.* 2007). This latest version 2.1 of the product was released in April 2020, and offers major improvements over the earlier version 2.0 from 1 January 2016 onwards, which includes broader incorporation of buoy and Argo float data to correct for satellite biases, enhanced satellite data input, refined bias correction algorithms, and revised sea-ice concentration conversion (Banzon *et al.* 2020). Prior to 1 January 2016, temperature and anomaly data in versions 2.0 and 2.1 are identical, but the file formats in version 2.1 have been updated from netCDF3 to netCDF4, along with the metadata (Huang *et al.* 2021*a*). The dataset commences on 1 September 1981, but here the last few months of 1981 have been truncated such that the period of our analysis commences from 1 January 1982 and ends at 31 December 2020.

Many observational SST products are available, but the primary requirements for the MHW analysis herein were high spatial and temporal resolution, over a long time span. Several products fulfill these requirements (Yang *et al.* 2021), but the DOISST dataset has been widely used in MHW studies, and it ranks highly for maturity in terms of documentation, storage, and dissemination (Yang *et al.* 2021). There are larger differences between different products in the early years of the satellite era (1982–2002), and although the NOAA DOISST product exhibits a cool bias in most regions, and in the global mean, the differences are small compared to the observational product ensemble median (Yang *et al.* 2021). Around Australia, there are slight cool biases off the northwest coast in the Indian Ocean, and in the Great Australian Bight, but the biases relative to the ensemble median are negligible in other regions around Australia (Yang *et al.* 2021). Biases and root-mean-square differences in the period 2016–2020 relative to measurements from all buoys and Argo floats are also low compared to other products (Huang *et al.* 2021*b*).

Given the relatively small differences between different observational products, it is expected that most would result in very similar MHW metrics. An analysis of coastal MHWs around the planet indicates that the largest differences occur in mean MHW intensities, with much smaller differences in all other metrics (Marin *et al.* 2021). Around Australia, most MHW metrics (aside from mean MHW intensities) are in agreement across products (Marin *et al.* 2021). The Marine Heatwaves Tracker (http://www.marineheatwaves.org/tracker.html) allows for comparison between three different observational products (DOISST, ESA SST CCI v2.1, and CMC). Some testing with that tool shows that although there are differences in the annual maximum MHW category, the spatial patterns tend to be largely in agreement. This study is not intended to be a comparison between observational products, but the public availability of the MHW metrics generated by this study may facilitate future comparison between MHW metrics from DOISST and other products.

A MHW is qualitatively defined as a discrete, prolonged, anomalously warm water event. We apply a quantitative definition following Hobday *et al.* (2016), where a MHW is a period during which the daily temperature exceeds the 90th percentile threshold, above a seasonally varying climatology, for at least five consecutive days. Two excursions above the threshold separated by less than 3 days are

considered a single event. Here the climatological period is chosen as 1983–2012, following the recommendation of Hobday *et al.* (2018). The climatological mean and 90th percentile threshold were computed over an 11-day window centred on each calendar day, sampling each year within the baseline period. After computing the mean and threshold for each calendar day, they were further smoothed by applying a 31-day moving mean.

Categorisations of MHW intensities are based on multiples of the local (spatial and temporal) difference between the climatological mean and the 90th percentile threshold (Hobday *et al.* 2018). In this way, intensities between $1\times$ and $2\times$ this value are denoted as Moderate, between $2\times$ and $3\times$ as Strong, between $3\times$ and $4\times$ as Severe, and $>4\times$ as Extreme.

The maximum intensity of a MHW is taken as the largest, single-day, temperature anomaly of the event, relative to the smoothed climatological mean. The duration is the period between first day of exceedance of the smoothed 90th percentile, and the day of departure below the threshold. The frequency is the average number of MHW events detected per year, and computed by counting the total number of events over a given period, then dividing by the number of years. The cumulative intensity of an event is the sum of the temperature anomaly, relative to the smoothed climatological mean, over each day of the event, given in units of °C days.

Since the maximum MHW intensity is identified as the largest temperature anomaly, seeking the strongest MHWs following this measure tends to return events that typically occur during the months of strongest SST variability, usually the summer months outside of the tropics, when departures from the seasonally varying climatology tend to be larger. The Hobday *et al.* (2018) MHW category definition accounts for this seasonal effect, since the category is a discrete multiple of the SST anomaly (SSTA) scaled by the seasonally varying difference between the 90th percentile threshold and the climatological mean. The continuous ratio has been referred to as 'severity' in some studies (e.g. Misra *et al.* 2021), i.e.

$$\text{Severity} = \frac{\text{SSTA}}{\text{Threshold} - \text{Climatology}}.$$

The maximum severity is thus simply the largest, single-day, normalised intensity during a MHW. This use of the maximum severity, as opposed to maximum intensity, avoids any seasonal bias in ranking the strongest MHW events. Note that the severity is a dimensionless index, whereas the usual definition of intensity is in units °C.

The Oceanic Niño Index (ONI) is used in reference to the El Niño–Southern Oscillation (ENSO) phase and magnitude. Data are provided by the NOAA Climate Prediction Center. The MHW metrics were computed using the *marineHeatWaves* python module, written by Eric C. J. Oliver and publicly available at: https://github.com/ecjoliver/marineHeatWaves.

The MHW metrics generated by this study, along with the code, are publicly available at: https://github.com/jbkajtar/mhw_australia.

3 MHWs in the Australian region

There is a considerable degree of variation in mean MHW metrics around different parts of Australia (Fig. 1). Over the period 1982–2020, there have been 2–3 MHWs per year on average across most of the region, but more than three events per year off the coasts of northwest and southeast Australia, and fewer than two events per year in the southwest (Fig. 1*a*). The spatial pattern of mean maximum intensity per MHW provides further details (Fig. 1*b*). The southeast exhibits the most intense MHWs, at >2.5°C above the climatological mean on average. The strong intensity MHWs in that region are associated with the western boundary current, namely the East Australian Current (EAC) and the EAC Extension south of ~33°S (Ridgway 1997, 2007). Western boundary currents in the subtropics transport heat poleward along the western margins of ocean basins, and typically exhibit strong temperature fronts and eddies, with large variability across a range of timescales (Holbrook *et al.* 2019). Southwest Australia also exhibits intense MHWs, despite markedly less frequent MHWs. Conversely, to the northwest of Australia, where MHW frequency is high, the mean intensity is lower than in the southeast and southwest. Mean MHW duration tells a different story (Fig. 1*c*). The longest events occur in the Tasman Sea, at close to 20 days on average, and the shortest events occur around Papua New Guinea and Indonesia. Despite the regional variations in MHW metrics, a common signature is that the Tasman Sea has tended to have more frequent, stronger, and longer MHWs than other locations around Australia.

Trends in MHW metrics also reveal that the Tasman Sea has been experiencing the largest increase in frequency, intensity, and duration over the past four decades, relative to other Australian region marine waters (Fig. 1*d–f*). The Tasman Sea has been deemed a global warming hotspot (Holbrook and Bindoff, 1997; Ridgway, 2007; Wu *et al.* 2012; Hobday and Pecl, 2014; Oliver *et al.* 2017). Frequency, intensity, and duration of MHWs have all trended sharply upward in the region over recent decades. There are some areas of negative trends, mostly seen in intensity (Fig. 1*e*), but they are much weaker in magnitude than in the regions experiencing positive trends. Time series of annual MHW metrics, averaged over the whole Australian region, similarly show positive trends (Fig. 1*g–i*). Annual MHW frequency (Fig. 1*g*) and duration (Fig. 1*i*) both show a clear increasing trend, but it is close to zero for intensity (Fig. 1*h*). The ENSO is a primary driver of MHWs around Australia, but other modes also play a role (Holbrook *et al.* 2019). As will be shown qualitatively in Section 4, El Niño drives MHWs in some regions, whereas La

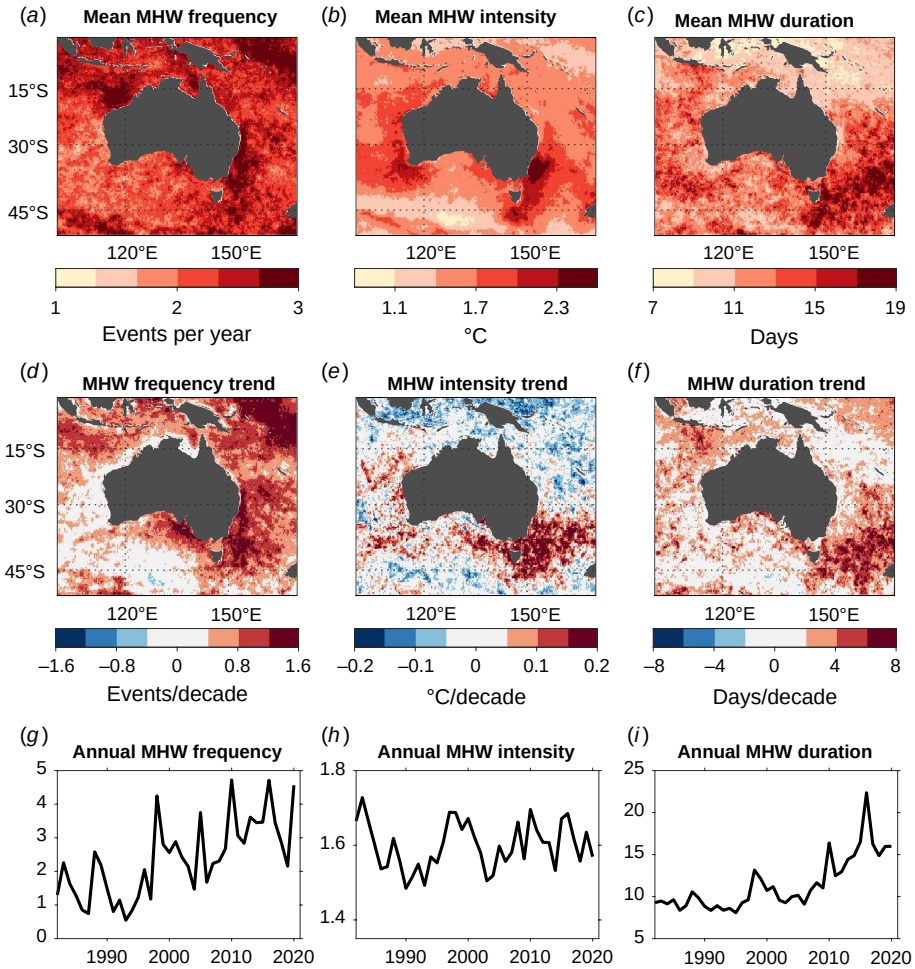

Fig. 1. Observed marine heatwave (MHW) metrics around Australia from 1982 to 2020. (*a–c*) Annual means of number of MHWs per year, maximum intensity (°C above climatology), and duration. (*d–f*) Linear trends of the same metrics shown in (*a–c*). (*g–i*) Annual time series of metrics shown in (*a–c*), area-averaged over the entire region.

Niña plays a greater role in others. There are notable peaks in the timeseries for MHW duration in 1988, 1998, 2010, and 2016 (Fig. 1*i*), all of which are years in which ENSO switched from El Niño to La Niña, but are furthermore linked to the extreme La Niñas in 1988/1989 and 2010/2011, and extreme El Niños in 1997/1998 and 2015/2016.

To illustrate that each MHW metric is not necessarily coupled, the years in which the strongest and longest MHWs around Australia occurred were analysed (Fig. 2). The strongest MHWs are taken to be those exhibiting the most intense single-day SST departure from climatology, and the longest MHWs as those with the longest period for which SST is above the 90th percentile threshold. The years in which the strongest (Fig. 2*a*) and longest (Fig. 2*b*) MHWs occurred do not necessarily coincide, and in fact rarely do. Only in some small regions, mostly off the coast of Western Australia or in the Tasman Sea, are they the same. The largest intensity MHWs appear to typically coincide with extreme ENSO events. The strongest MHWs in the south, and in a scattering of other areas, coincide with the 1982/1983 El Niño (dark blue), the far southwest and far northwest with the 1998/1999 La Niña (teal), the Western Australian coastal region with the 2010/2011 La Niña (dark yellow), and the Tasman Sea with the extreme 2015/2016 El Niño (gold; Fig. 2*a*). With some minor exceptions, the longest duration events have mostly occurred since 2010 (Fig. 2*b*).

Maximum MHW intensities of the strongest events have exceeded +5°C in parts of the Tasman Sea and off Western Australia (Fig. 2*c*). These areas mostly align with the small regions where the strongest and longest MHWs tend to coincide, which can also be seen by comparing with the maximum intensities for the longest duration MHWs (Fig. 2*d*). Intensities exceeding +5°C are exceptionally rare, and most of the seas around Australia have not experienced SSTs more than 3°C above normal (Fig. 2*c*). The longest MHWs around Australia have exceeded 200 days in duration, and they have occurred primarily in the Tasman Sea, and near the island of Java in the northwest (Fig. 2*f*). It is rare for MHWs in the Australian region to exceed 100 days in duration, with some parts of the north-east not having experienced MHWs of duration longer than 50 days over this observational period. The difference in duration of the strongest and longest MHWs is substantial (cf. Fig. 2*e*, *f*).

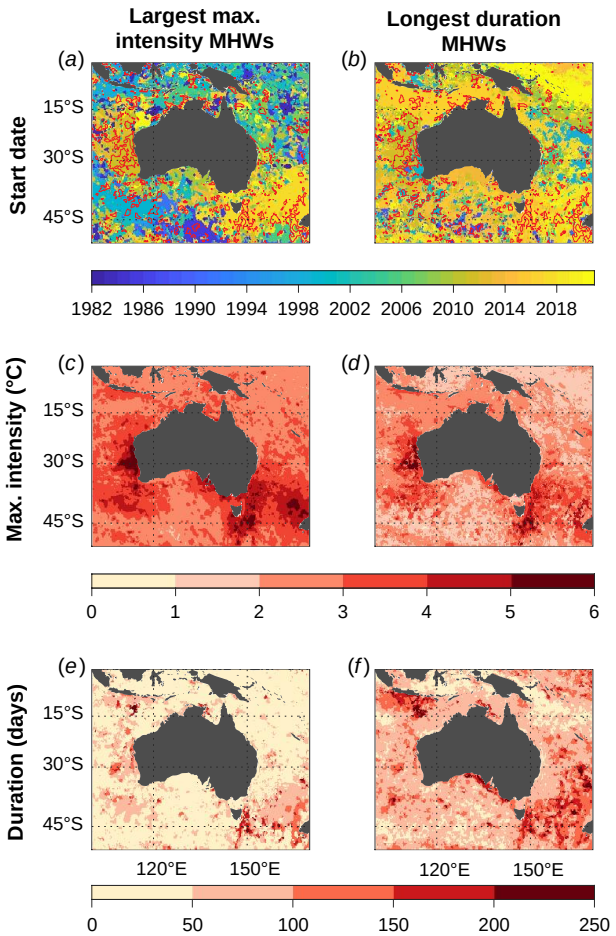

Fig. 2. Distribution of the strongest and longest observed marine heatwaves (MHWs), on a 0.25° grid-point basis. (*a*) Start date (year) of the strongest MHW, determined as being the event with the largest maximum intensity (in °C) above climatology. (*b*) Start date (year) of the longest duration MHW in days. Small areas enclosed by red lines in (*a*) and (*b*) denote where the strongest and longest MHWs are the same event. (*c*, *d*) Maximum intensity (°C) observed in the strongest and longest events indicated in (*a*) and (*b*). (e, *f*) Duration (days) of the strongest and longest events indicated in (*a*) and (*b*).

Another useful metric of MHWs is the category of intensity (Hobday *et al.* 2018). The mean numbers of days per year spent in Moderate, Strong, Severe, or Extreme categories, in two 20-year periods, again demonstrate increasing MHW exposure days around Australia (Fig. 3). The mean number of Moderate MHW days per year increased substantially in the period 2001–2020 relative to 1982–2001 (cf. Fig. 3*a*, *b*). There is likely to be greater uncertainty in the data in the earlier period, since there is less agreement between observational SST products prior to 2000 (Rayner *et al.* 2019), but the trend in MHW days is nevertheless clear. In the more recent period, there were at least 10 Moderate MHW days per year on average at every grid-point, with most experiencing >30 days per year (Fig. 3*b*). In contrast, almost nowhere experienced more than 30 MHW days per year in the earlier period (Fig. 3*a*). Similarly, the number of Strong and Severe MHW days per year have increased over the two periods (Fig. 3*c–f*). The changes are less clear for Extreme MHW days, since they have been rare (Fig. 3*g*, *h*). The timeseries of the fraction of ocean around Australia reaching maximum categories reinforces the finding that the number of Strong and Severe MHW days in particular is increasing, and the fraction of ocean not experiencing a MHW is decreasing (Fig. 3*i*).

Since 1982, only very few areas have experienced the Extreme category of MHWs, and mainly only in the southern part of the region, including parts of the Tasman Sea, off the coast of Western Australia, in the Great Australian Bight, and in the Southern Ocean (Fig. 4). Several areas have not registered Severe MHWs, with Strong being the highest category observed. This is largely the case in the Coral Sea and the GBR. Despite the fact that the GBR has experienced three MHWs in recent years, which resulted in extensive ecological damage (Hughes *et al.* 2019; Bureau of Meteorology 2020), very few parts of the GBR have experienced Severe category MHW days. An Extreme MHW in the GBR, should one occur, would therefore likely cause widespread devastation. The features in Fig. 4 are evident in the spatial pattern for the global domain shown by Sen Gupta *et al.* (2020), despite using different versions of the NOAA DOISST data, and slightly different periods of analysis.

4 MHWs in case study regions

Here we more closely analyse the four marine case study regions discussed in the introduction and by McInnes *et al.* (2021), but add a fifth region (the South Australian Basin). The case study regions are indicated in Fig. 4. For each of the five identified regions, the SST in the domain was first area-averaged, and the MHW metrics then computed from the resulting daily time series. The time series of annual MHW days is presented in the following subsections, with an indication of the number of days spent in each MHW category. The strongest MHWs (by maximum intensity, maximum severity, and cumulative intensity) and longest MHWs are identified, and the time series of some selected events are plotted. As shown earlier, the strongest and longest MHWs are not necessarily the same event, but in some regions they are.

The bounds of the selected case study regions (justified in the respective sections that follow) are:

- Western Australia: 110–116°E, 32.5–22°S.
- Torres Strait: 132–148°E, 18–9°S.
- Great Barrier Reef: 142–155°E, 25–10°S.
- Tasman Sea: 147–157°E, 46–37°S.
- South Australian Basin: 132–143°E, 40–31°S, but with the southwest corner trimmed along the line between 132°E, 35°S and 143°E, 31°S.

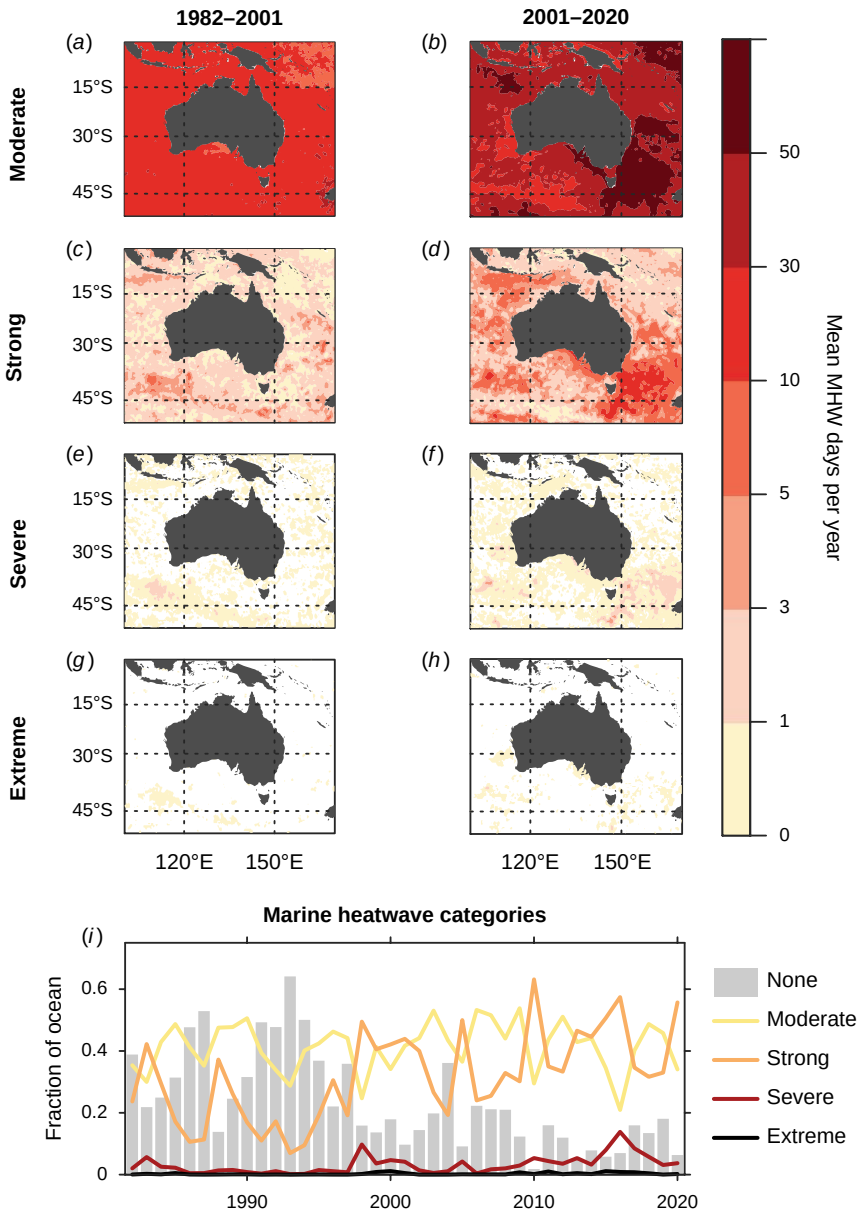

Fig. 3. Observed annual mean days duration in each marine heatwave (MHW) category. (*a–h*) Mean MHW days per year in two overlapping 20-year periods, following the MHW categorisation scheme of Hobday *et al.* (2018). Note that here the counts of Moderate MHW days include the numbers of days spent in any higher MHW category, and likewise for Strong and Severe MHW day counts. (*i*) Area of maximum MHW category recorded, per year, as a fraction of the ocean area depicted in (*a–h*).

A shortcoming of this widely used area-averaged approach is that the MHW metrics are sensitive to the particular domains selected for each region. Hence, if a significant MHW occurred slightly outside the domain, or straddled the boundary, then it may not be identified as one of the strongest or longest MHWs. However, the regions were generally selected based on the spatial extent of major MHWs identified in the literature, and hence there is a historical context for the choices that were made.

Although only the top three ranked MHWs by duration, maximum intensity, maximum severity, and cumulative intensity are discussed in the following sections, the publicly available dataset allows for further analysis. For example, analysis that may be more relevant to impact studies is the spatial pattern of MHW exposure days in a given year for a selected region. Although the dataset is not exhaustive, such a metric is readily available.

4.1 Western Australia

Hobday *et al.* (2018) identified two MHWs in the Western Australian region, one during 1999 classified as Severe (Category 3), and another in 2011 classified as Extreme (Category 4). The region selected here is similar to that used by Hobday *et al.* (2018), but extended farther to the north to include Shark Bay, which is World Heritage listed on the basis of its 'outstanding universal value' (NESP Earth Systems and Climate Change Hub 2018*a*).

Averaging over the Western Australia region (110–116°E, 32.5–22°S), the maximum MHW category observed is

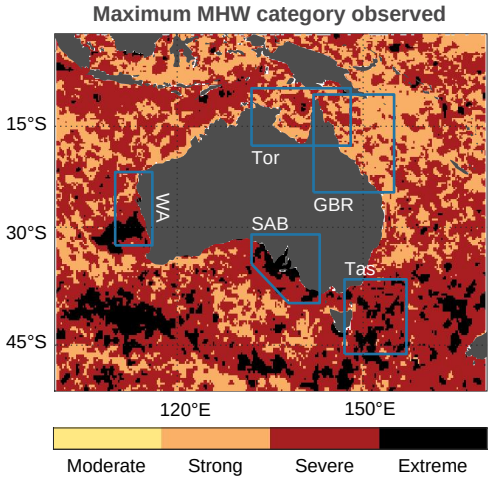

Fig. 4. Maximum marine heatwave (MHW) category registered at each grid-point over the period analysed (1982–2020). Case-study regions in Section 4 are indicated by blue rectangles: Western Australia (WA), Torres Strait (Tor), Great Barrier Reef (GBR), Tasman Sea (Tas), and the South Australian Basin (SAB).

Severe, in 2011, but Strong MHWs have occurred in several other years (Fig. 5). The discrepancy in the categorisation of the 2011 MHW, here as Severe, and Extreme by Hobday *et al.* (2018), is due to the fact that a larger region has been analysed in the present study, diminishing some of the large anomalies in the area-averaged SST. There have also been extended periods with no recorded MHWs, such as 1990–1994, 2001–2008, and 2016–2018. During these periods, several marine cold spells occurred (Feng *et al.* 2021). Holbrook *et al.* (2019) identified a link between La Niña and MHWs in this region (see their Supplementary fig. 3*b*), and that link is apparent here. The strongest La Niña events occurred in 1988/1989, 1998/1999, 2007/2008, and 2010/2011 (Feng *et al.* 2013), and were all followed by elevated counts of MHW days (Fig. 5*a*). The high MHW day counts in 1989, 1999, and 2011 corresponded with the strongest Ningaloo Niño events, which is an episodic occurrence of warm ocean conditions along the subtropical coast of Western Australia (Kataoka *et al.* 2014, 2017; Feng *et al.* 2015; Marshall *et al.* 2015; Zhang *et al.* 2018). These Ningaloo Niño events were coincident with three of the four largest La Niña events (Kataoka *et al.* 2014; Feng *et al.* 2015).

For the selected case study region, the longest MHW occurred in 1999 and persisted for 146 days (Fig. 5*b*). Its maximum intensity was 2.2°C above normal, ranking it 5th by event with most intense single-day anomaly, but 3rd by maximum severity (i.e. accounting for seasonal variability). The event had the largest cumulative intensity (183.5°C days), which is unsurprising given that longer duration usually results in greater cumulative intensity. It was classified as Strong for a period during July–August 1999. As noted earlier, Hobday *et al.* (2018) also identified this event, but found that it briefly entered the Severe category. This discrepancy is primarily due to the larger northward extent of this region selected here. Nevertheless, the two time series that characterise the event are similar (c.f. Fig. 5*b* and Hobday *et al.* 2018; their fig. 3*f*). Hobday *et al.* (2018) reported that they were unable to locate any studies that linked ecological impacts with this event.

The strongest MHW in this region occurred in 2011 (Fig. 5*c*). It ranks 1st in both maximum intensity (4.1°C above average) and maximum severity, but also ranks 3rd in duration (63 days). Again, there are strong similarities with the timeseries shown by Hobday *et al.* (2018; their fig. 3*j*), who show that the event was classified as Extreme (Category IV) for 12% of its duration. For the broader region selected here, the maximum classification is Severe (Category III). The anomalously warm ocean temperatures were largely driven by poleward advection of warmer tropical water, enhanced by a weakened northward Capes Current, and air–sea heat flux into the ocean (Pearce and Feng 2013; Benthuysen *et al.* 2014). The 2011 Western Australian MHW, arguably the most extreme Australia has experienced, was associated with widespread impacts. Based on field studies and satellite estimates, Shark Bay experienced damage to about 36% of its extensive seagrass meadows (Arias-Ortiz *et al.* 2018), including dieback (>90% in some areas), which have ecosystem-function, cultural, and economic significance, and led to closures in the scallop and crab fisheries (Thomson *et al.* 2015; Caputi *et al.* 2019). A range of seaweed species became regionally extinct (Smale and Wernberg 2013; Wernberg *et al.* 2013, 2016), and kelp forests died back and were replaced by turf-forming algae (Wernberg *et al.* 2013, 2016). Corals were severely impacted (Abdo *et al.* 2012; Moore *et al.* 2012) along with invertebrate species (Caputi *et al.* 2016). The heatwave had a lasting effect on the region, and after several years, only parts of the ecosystem have shown reasonable recovery (Caputi *et al.* 2019).

While the iconic 2011 MHW commenced on 4 February 2011, based on the MHW definition applied here, it was preceded by another notable event (Fig. 5*c*, Table 1) spanning 15 October 2010 to 30 January 2011. This earlier event ranks 2nd by duration and cumulative intensity, and 3rd and 4th for maximum intensity and severity, respectively. The unusually warm conditions prior to the 2011 MHW likely exacerbated the ecological devastation.

The 2nd strongest MHW by maximum intensity occurred in 2012, which ranks 6th and 7th for duration and maximum severity respectively (Fig. 5*d*). This event was identified by Feng *et al.* (2015) and Holbrook *et al.* (2019), but associated ecological impacts do not appear to be recorded, perhaps due to the widespread devastation of the 2011 event that preceded it by less than a year. The metrics of the four events discussed here, along with another MHW that occurred in 2015, are shown in Table 1. These five events together account for the top three ranking events in each metric shown.

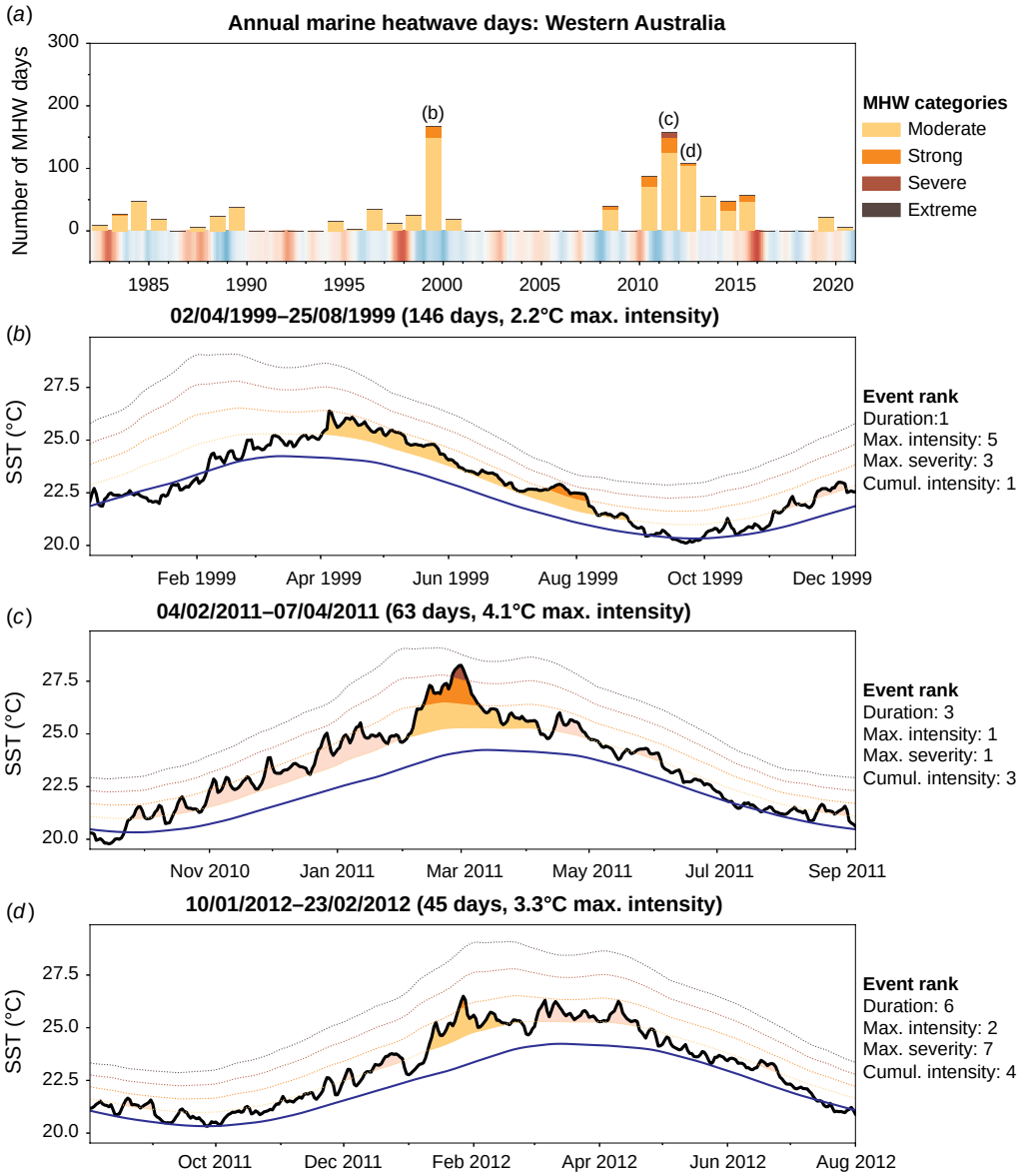

Fig. 5. Western Australian marine heatwaves (MHWs), in the domain bounded by 110–116°E, 32.5–22°S (as shown in Fig. 4). (*a*) Annual counts of days observed in each MHW category, shown as stacked bars. The Oceanic Niño index, representing ENSO, is plotted as shades of red (El Niño) and blue (La Niña), where more intense colours indicate stronger phases. (*b–d*) Timeseries of some of the major MHWs in the region. In each panel, the blue curve denotes the smoothed climatological mean, the black curve is the area-averaged SST timeseries for the domain, and the yellow, orange, red, and dark red curves denote the levels for Moderate, Strong, Severe, and Extreme categorisation, respectively. The MHW events of particular interest during the period are colour shaded according to their category reached, and pink shading denotes MHWs other than the event being highlighted in each panel.

4.2 Torres Strait

Benthuysen *et al.* (2018) identified a MHW off the coast of Northern Australia in 2016. They analysed five boxed regions, but since here the focus is the Torres Strait region in particular, a smaller subregion of their domain was chosen. The bounds of the domain selected here are 132–148°E, 18–9°S, which align with the extent of the Gulf of Carpentaria and Torres Strait boxed regions together, as used by Benthuysen *et al.* (2018). This 2016 MHW was also identified in other studies, each of which used slightly different regions of analysis (Hobday *et al.* 2018; Oliver *et al.* 2018*b*).

The time series of annual counts of MHW days shows that MHWs have occurred in most years in the region (Fig. 6). Several years have also experienced Strong category MHWs.

Table 1. List of major marine heatwaves in the Western Australian case study region. For each event, the start and end dates are noted, along with its total duration, maximum single day intensity, maximum single day severity, and cumulative intensity. The rank of the event for each metric, among all events in the region over the observed period, is given in parentheses. The table lists at least the top three ranked events for each metric.

Dates (dd/mm/yyyy)	Duration (days)	Maximum intensity (°C)	Maximum severity	Cumulative intensity (°C days)
02/04/1999–25/08/1999	146 (1)	2.23 (5)	2.72 (3)	183.5 (1)
15/10/2010–30/01/2011	108 (2)	2.78 (3)	2.66 (4)	178.3 (2)
04/02/2011–07/04/2011	63 (3)	4.13 (1)	3.56 (1)	150.0 (3)
10/01/2012–23/02/2012	45 (6)	3.30 (2)	2.37 (7)	86.4 (4)
20/09/2015–02/11/2015	44 (7)	1.89 (15)	2.82 (2)	56.0 (6)

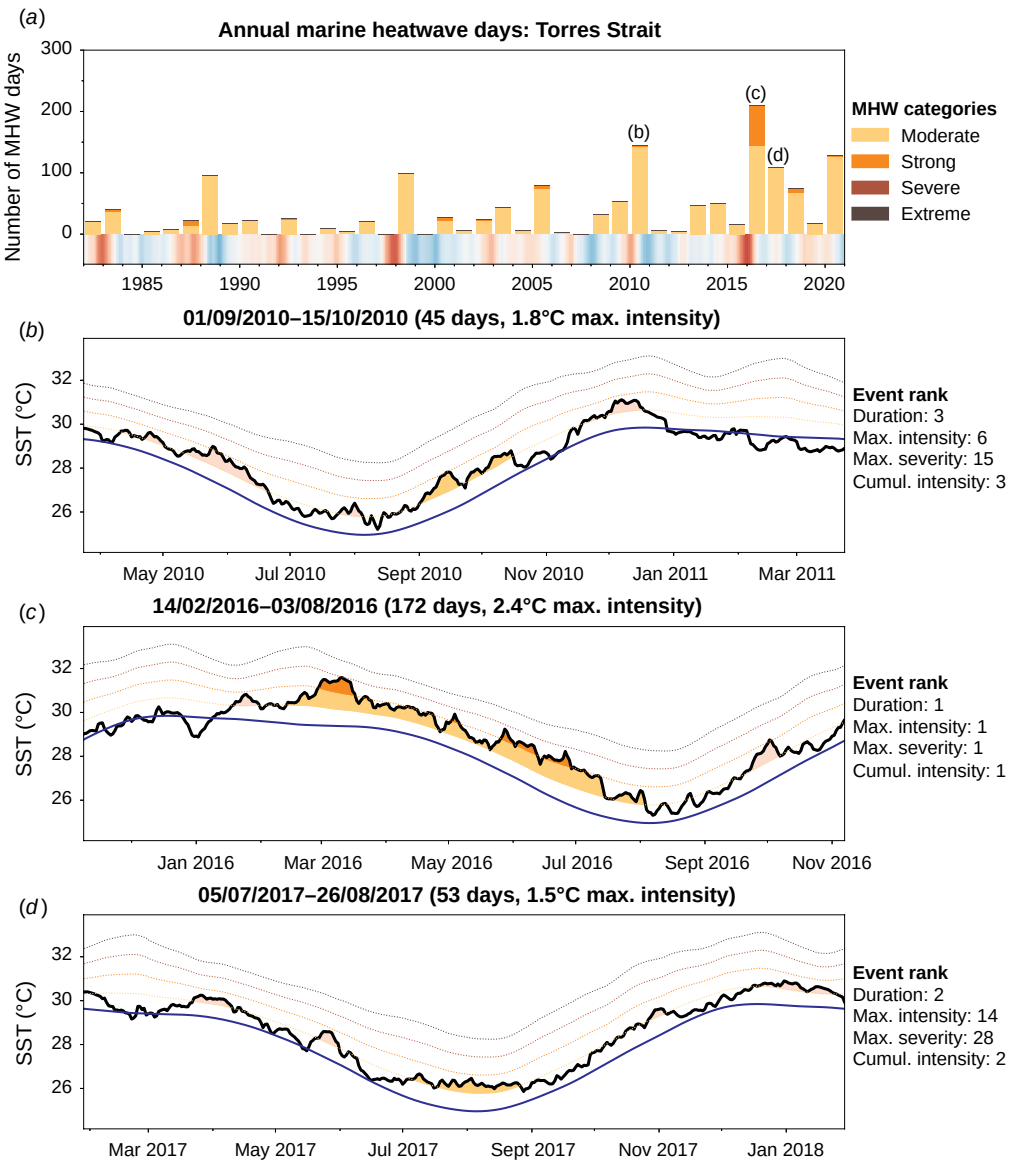

Fig. 6. As in Fig. 5, but for Torres Strait marine heatwaves (MHWs), in the domain bounded by 132–148°E, 18–9°S (as shown in Fig. 4).

While no statistically significant correlation at zero lag was found with ENSO by Holbrook *et al.* (2019), it appears as though there is some lagged relationship with El Niño, since the 1982/1983, 1997/1998, 2009/2010, and 2015/2016 El Niño events were all followed by increased MHW days in the following year (Fig. 6*a*).

In 2010, there were ~150 MHW days recorded (the second highest behind 2016). The longest duration MHW that year lasted 45 days, which was the 3rd longest and 3rd strongest by cumulative intensity, but only the 6th and 15th strongest with respect to maximum intensity and severity, respectively (Fig. 6*b*).

Undoubtedly the most extreme MHW in the region occurred in 2016 (Fig. 6*c*). It ranks 1st for duration, maximum intensity, severity, and cumulative intensity, falling just short of Severe classification (Table 2) and persisting for 172 days. Elevated ocean temperatures first arose in the southeast tropical Indian Ocean in November 2015, and propagated eastward toward the Coral Sea (Benthuysen *et al.* 2018). The MHW co-occurred with an extreme El Niño and weakened monsoon activity, which acted to enhance air–sea heat flux into the ocean (Benthuysen *et al.* 2018). In 2016, a quarter of the global ocean surface experienced either the most intense or longest duration MHW (Oliver *et al.* 2018*b*), which were due to the influence of the preceding extreme El Niño.

Widespread coral bleaching was reported in the GBR as a result of the 2016 MHW (GBRMPA 2016; Hughes *et al.* 2017), along with mangrove die-back (Duke *et al.* 2017; Harris *et al.* 2017) and reduced mud crab fishery capacity (NTSC 2016). Indigenous communities and fishers strongly depend on marine resources in the Torres Strait (NESP Earth Systems and Climate Change Hub 2018*b*), and they were the first to notice the impacts. The Anindilyakwa Rangers reported the bleaching of giant clams near Groote Eylandt, and the Crocodile Island Rangers shared reports of coral bleaching at Murrungga Island (Wild 2016).

Apart from the 2016 MHW, there is considerable variation in the rank of other MHWs that have occurred in the Torres Strait. The 2nd ranked MHW by maximum severity occurred during the summer of 1986/1987, but lasted only 16 days (ranked 24th), and exhibited a maximum intensity of 1.7°C (ranked 8th; Table 2). The 2nd ranked MHW by maximum intensity occurred in 2005, reaching 2.2°C above climatology. It lasted 20 days (ranked 14th) but registered a Strong classification (ranked 3rd by maximum severity; Table 2). Finally, the 2nd ranked MHW by duration occurred in 2017 and persisted for 53 days (Fig. 6*d*), well short of the 2016 MHW of 172 days. It ranks 14th and 28th for maximum intensity and severity respectively (Table 2).

4.3 Great Barrier Reef

The bounds for the Great Barrier Reef (GBR) were selected such that the northwest and southeast corners align closely with the extent of the GBR Marine Park (GBRMP; GBRMPA 2004). The bounds of the domain are 142–155°E, 25–10°S.

Three years during the observational period have experienced approximately 200 MHW days: 1998, 2010, and 2016, all of which were associated with and/or followed El Niño events (Fig. 7*a*). Along with 2017 and 2020, these 5 years had substantially more MHW days than any other. The longest continuous MHW to date in this region, of 116 days duration, occurred in 1998 (Fig. 7*b*) following the extreme El Niño of 1997/1998 (McPhaden 1999). It is also the strongest event by cumulative intensity to date. Somewhat paradoxically, the MHW was partly driven by upwelled cooler water, but representing positive thermal anomalies, advected from the equatorial Pacific (Schiller *et al.* 2009; Berkelmans *et al.* 2010). Lower than average wind stress and extended periods of cloudless skies also contributed to the warmer than usual conditions (Schiller *et al.* 2009). During 1998, likely in combination with additional MHWs occurring before and after the 116-day event, approximately 87% of inshore coral reefs and 28% of offshore corals reefs were bleached to some extent (Berkelmans and Oliver 1999). The strongest MHW by maximum severity occurred in 2010 (Fig. 7*c*), but the warmest temperature anomalies occurred during the cool season, perhaps minimising any ecological impacts. The 2010 MHW is also the 3rd longest on record.

The 2016 MHW, which spanned a large area of the GBR (Hobday *et al.* 2018), emerged in the months following the peak of the MHW in the Torres Strait and tropical north of Australia (Fig. 7*d*). This is the 2nd longest recorded event for the GBR, at 101 days, and elevated temperatures had already been recorded for the region in the months prior

Table 2. As in Table 1, but for major marine heatwaves in the Torres Strait case study region.

Dates (dd/mm/yyyy)	Duration (days)	Maximum intensity (°C)	Maximum severity	Cumulative intensity (°C days)
31/12/1986–15/01/1987	16 (24)	1.70 (8)	2.60 (2)	21.6 (18)
21/02/2005–12/03/2005	20 (14)	2.15 (2)	2.45 (3)	27.4 (9)
01/09/2010–15/10/2010	45 (3)	1.81 (6)	1.99 (15)	56.1 (3)
14/02/2016–03/08/2016	172 (1)	2.35 (1)	2.97 (1)	238.1 (1)
19/09/2016–06/10/2016	18 (21)	1.87 (3)	2.07 (12)	24.7 (12)
05/07/2017–26/08/2017	53 (2)	1.50 (14)	1.80 (28)	59.1 (2)

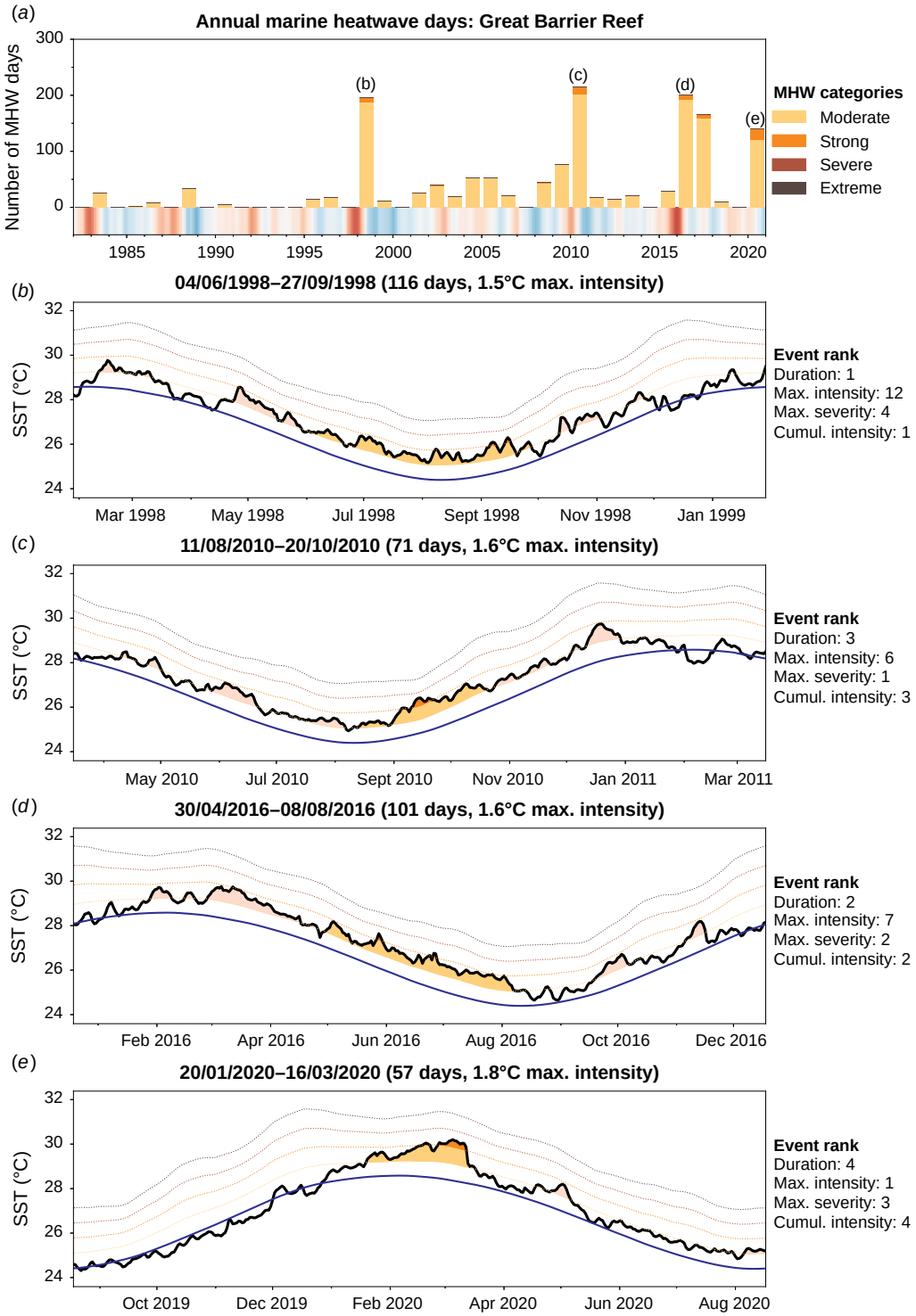

Fig. 7. As in Fig. 5, but for Great Barrier Reef marine heatwaves (MHWs), in the domain bounded by 142–155°E, 25–10°S (as shown in Fig. 4).

to its commencement (Fig. 7*d*). It is ranked 7th and 2nd for the maximum intensity and severity, respectively, and 2nd for cumulative intensity. As noted earlier, the 2016 MHW in the Torres Strait had already been associated with coral bleaching in the northern GBR, but this broader extension of the warming pattern led to extensive and severe bleaching, and some mortality, across the entire GBR (GBRMPA 2017; Hughes *et al.* 2017).

Table 3. As in Table 1, but for major marine heatwaves in the Great Barrier Reef case study region.

Dates (dd/mm/yyyy)	Duration (days)	Maximum intensity (°C)	Maximum severity	Cumulative intensity (°C days)
04/06/1998–27/09/1998	116 (1)	1.46 (12)	2.36 (4)	114.0 (1)
17/11/2008–23/12/2008	37 (7)	1.82 (2)	2.07 (7)	48.4 (7)
11/08/2010–20/10/2010	71 (3)	1.59 (6)	2.58 (1)	78.9 (3)
12/12/2010–29/12/2010	18 (23)	1.67 (3)	1.90 (12)	24.0 (15)
30/04/2016–08/08/2016	101 (2)	1.59 (7)	2.45 (2)	109.8 (2)
20/01/2020–16/03/2020	57 (4)	1.84 (1)	2.44 (3)	70.6 (4)

The strongest MHW by maximum intensity, at 1.8°C above average, occurred early in 2020. It is ranked 3rd by maximum severity and 4th by duration and cumulative intensity (Fig. 7*e*, Table 3). It was likely triggered by the very strong positive Indian Ocean Dipole event in the preceding months (Bureau of Meteorology 2020). Three summers on the GBR since 2015 have experienced mass coral bleaching (Bureau of Meteorology 2020), and despite only very small areas reaching the Severe category (Fig. 4), no region-wide MHWs have been registered as Severe overall.

4.4 Tasman Sea

The Tasman Sea region selected here encompasses the two different regions used by Oliver *et al.* (2017) and Hobday *et al.* (2018), extending farther north than the former, and farther south and east than the latter. The Tasman Sea domain analysed here is 147–157°E, 46–37°S.

The Tasman Sea has exhibited substantial warming in recent decades, and is considered a global warming hotspot (Holbrook and Bindoff 1997; Ridgway 2007; Hobday and Pecl 2014; Oliver *et al.* 2017), along with its coastlines (Marin *et al.* 2021). This is apparent in the trend in MHW days since 1982, with very few MHW days before 1998, and each year since 2013 has experienced some Strong category days (Fig. 8*a*). It is no surprise then that the strongest and longest MHWs in the Tasman Sea have occurred in recent years. Two events in particular have drawn much attention.

The MHW of the summer of 2015/2016 is the longest on record, at 318 days. It also ranks 2nd for maximum intensity at +2.9°C, and 2nd for maximum severity after briefly registering a Severe classification (Fig. 8*a*, Table 4). The event was the strongest by a large margin in terms of cumulative intensity (Table 4). During the 2015/16 MHW, SST was 2°C above average over an area about seven times the size of Tasmania, and reaching +3°C across an area about half the size of Tasmania (Oliver *et al.* 2017). The anomalous warming was driven by an intensified EAC Extension, transporting significantly more heat from the tropics into the region than usual (Oliver *et al.* 2017). Apart from the appearance of marine species normally residing farther north, the heatwave caused severe ecological impacts. There was an outbreak of Pacific Oyster Mortality Syndrome, leading to the closure of local hatcheries, and a decimation of juvenile Pacific Oyster stocks (Ugalde *et al.* 2018). Poor Blacklip Abalone condition was recorded during the event, with approximately 5% mortality. Reduced performance in cultured Atlantic Salmon resulted in a limited supply to seafood markets (Oliver *et al.* 2017; Hobday *et al.* 2018).

The 2nd longest MHW occurred less than 12 months after the 2015/2016 event. It persisted for 172 days, but ranks 4th and 5th for maximum intensity and severity, respectively (Fig. 8*c*). The other MHW to attract considerable attention was the 2017/2018 event, which ranks 1st for both maximum intensity and severity, and 4th for duration and cumulative intensity (Fig. 8*d*). SST of 3°C above average was recorded over a much wider area than the 2015/2016 MHW, and the unusual warmth extended across the Tasman Sea between Tasmania and New Zealand (Perkins-Kirkpatrick *et al.* 2019). Rather than a change in currents, this event was driven primarily by enhanced local air–sea heat flux, due to a strong high pressure system sitting over the region for many weeks (Perkins-Kirkpatrick *et al.* 2019). It has been shown that it was virtually impossible for the MHW to occur without the influence of human-induced global warming (Perkins-Kirkpatrick *et al.* 2019). The heatwave resulted in another outbreak of Pacific Oyster Mortality Syndrome, exacerbated by the temperature stress (Perkins-Kirkpatrick *et al.* 2019).

The strength of the changes observed in the Tasman Sea in recent decades, and its coupling to global warming, is an area of active research. Recent studies have made important advances in understanding the extent to which MHWs in the region are driven by currents, patterns of synoptic weather and climate variability, and large-scale atmosphere and ocean dynamics (Oliver *et al.* 2017; Oliver and Holbrook 2018; Holbrook *et al.* 2019; Perkins-Kirkpatrick *et al.* 2019; Li *et al.* 2020).

4.5 South Australian Basin

The South Australian Basin region was selected as a case study primarily due to the large area recording a MHW with a maximum severity of Extreme (Fig. 4). This analysis is partly aimed at revealing characteristics of that event, such as its timing, intensity, and duration. The selected region is bounded by 132–143°E, 40–31°S, but with the southwest

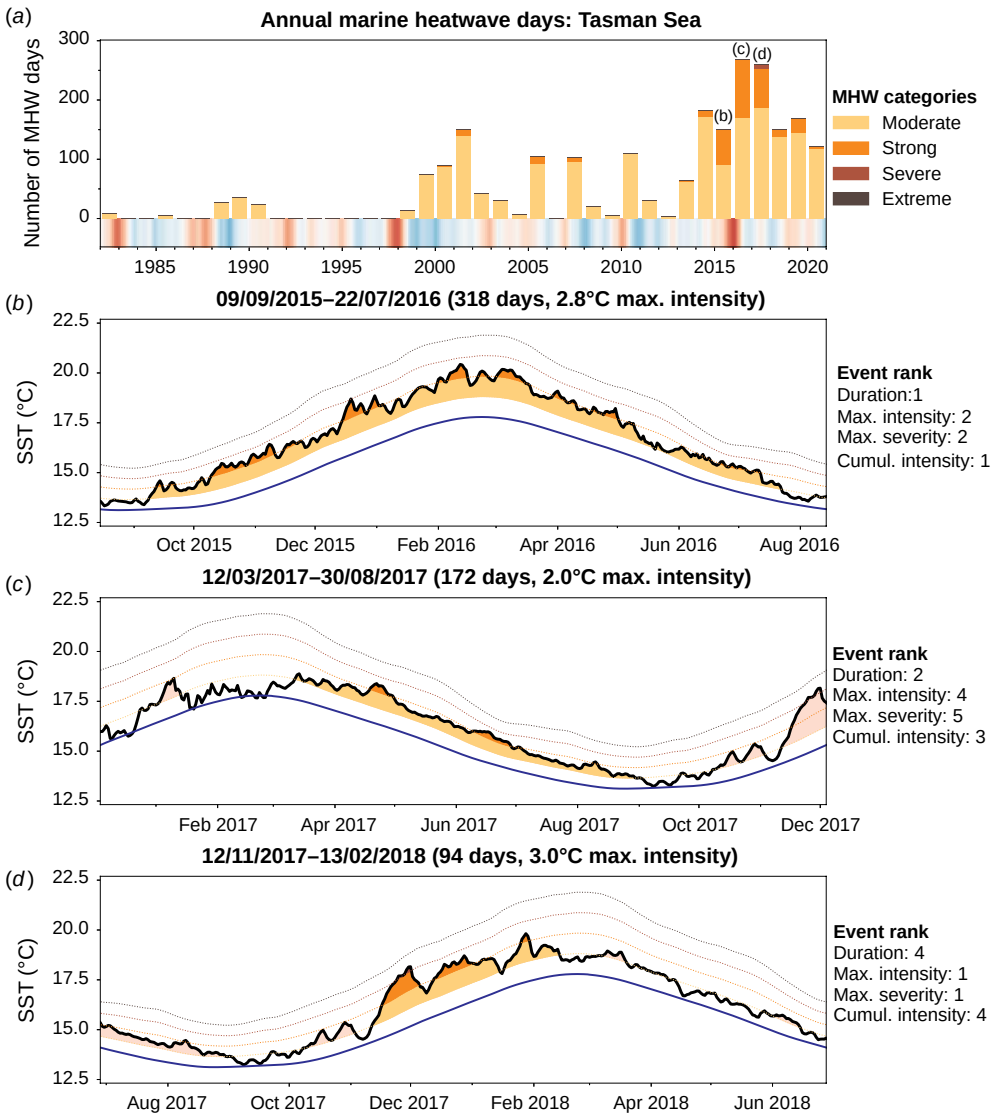

Fig. 8. As in Fig. 5, but for Tasman Sea marine heatwaves (MHWs), in the domain bounded by 147–157°E, 46–37°S (as shown in Fig. 4).

Table 4. As in Table 1, but for major marine heatwaves in the Tasman Sea case study region.

Dates (dd/mm/yyyy)	Duration (days)	Maximum intensity (°C)	Maximum severity	Cumulative intensity (°C days)
03/09/2001–15/10/2001	43 (10)	1.44 (32)	2.56 (3)	42.1 (13)
09/09/2015–22/07/2016	318 (1)	2.80 (2)	3.01 (2)	505.9 (1)
12/03/2017–30/08/2017	172 (2)	2.02 (4)	2.55 (5)	206.1 (3)
12/11/2017–13/02/2018	94 (4)	3.02 (1)	3.28 (1)	175.6 (4)
07/12/2018–26/04/2019	141 (3)	2.46 (3)	2.55 (4)	224.4 (2)

corner trimmed along the line between 132°E, 35°S and 143°E, 31°S.

In the region-wide average, the Extreme MHW category was detected to have occurred over a few days in November 2009. That short 21-day MHW ranks only 17th for duration, but 1st for both maximum intensity and severity (Fig. 9*b*). Since the event occurred in the climatologically cooler months, with relatively low cumulative intensity (Table 5),

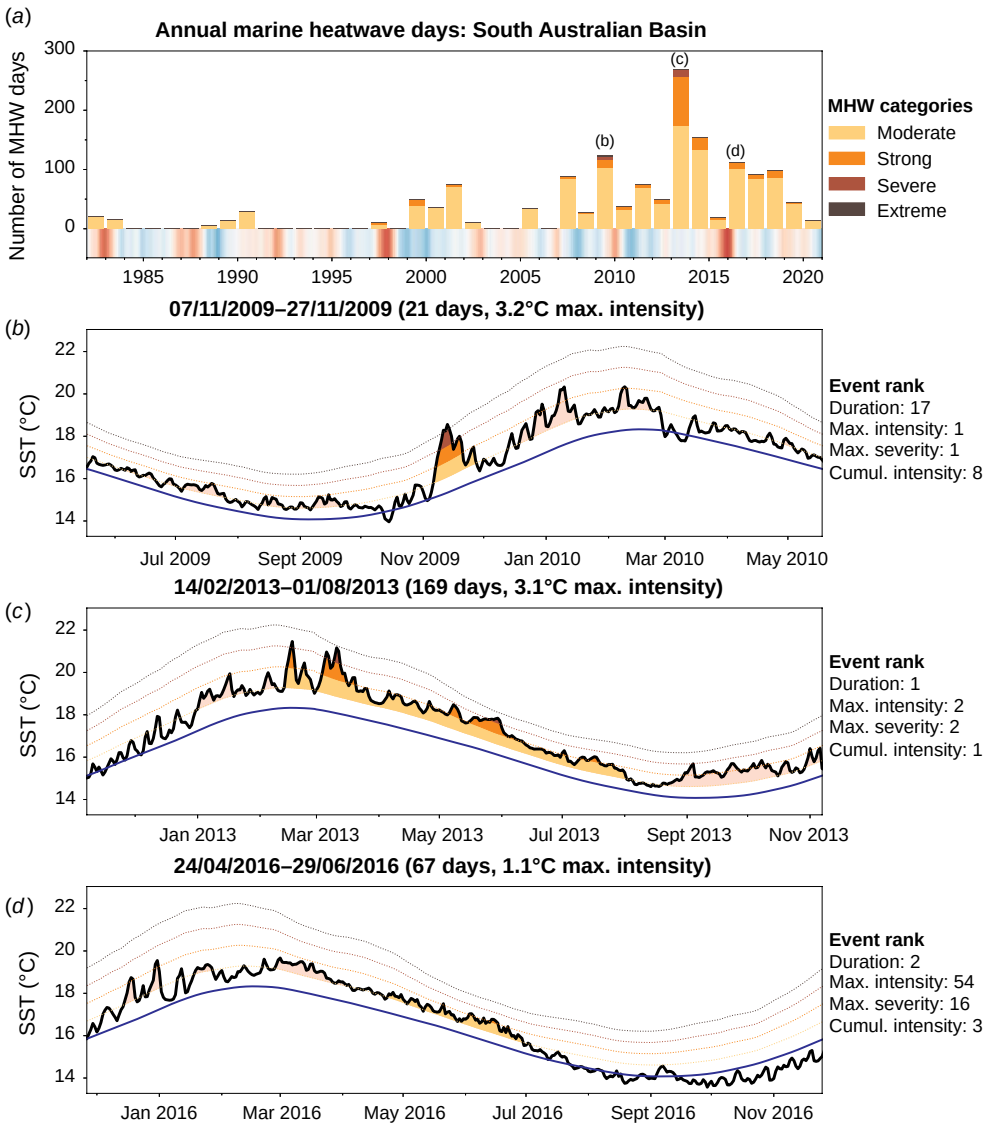

Fig. 9. As in Fig. 5, but for South Australian Basin marine heatwaves (MHWs), in the domain bounded by 132–143°E, 40–31°S (as shown in Fig. 4).

Table 5. As in Table 1, but for major marine heatwaves in the South Australian Basin case study region.

Dates (dd/mm/yyyy)	Duration (days)	Maximum intensity (°C)	Maximum severity	Cumulative intensity (°C days)
07/11/2009–27/11/2009	21 (17)	3.22 (1)	4.34 (1)	42.1 (8)
14/02/2013–01/08/2013	169 (1)	3.13 (2)	3.87 (2)	221.7 (1)
20/08/2013–22/10/2013	64 (3)	1.61 (29)	2.98 (4)	70.2 (2)
24/04/2016–29/06/2016	67 (2)	1.14 (54)	2.31 (16)	55.1 (3)
15/01/2018–30/01/2018	16 (29)	3.06 (3)	3.10 (3)	30.8 (15)

it likely had little impact on the local ecology, although its effect on seasonal-specific processes occurring at that time, such as reproduction, recruitment, or predator–prey interactions, remain unknown and require further research.

The largest number of MHW days observed in any single year in the South Australian Basin occurred during 2013, with over 250 MHW days detected (Fig. 9*a*). The largest contribution came from the most substantial MHW

occurring in that region (Fig. 9*c*), which ranks 1st for duration (169 days) and cumulative intensity, and 2nd for both maximum intensity and severity. During the earlier months of 2013, mortality of abalone and a range of fish species were recorded, and the MHW promoted blooms of harmful algae (Roberts *et al.* 2019). No other event has persisted anywhere near as long in the region, with the next longest event lasting 67 days, and with substantially weaker maximum intensity and severity (Fig. 9*d*, Table 5).

A recent study found that interannual southward shifts in the prevailing southern hemisphere mid-latitude westerly winds can play a role in ocean surface warming events in the South Australian Basin (Duran *et al.* 2020). That study also found that in CMIP5 21st century projections, wind trends might play a comparable role to radiative warming in driving ocean temperature trends.

5 Potential predictability of SST and MHWs

Recent advances in understanding the physical drivers of MHWs (Holbrook *et al.* 2019) provide an opportunity to explore their predictability. Predictability of MHWs is discussed in a Perspectives piece (Holbrook *et al.* 2020*b*), in which the large-scale climate drivers, teleconnections, and local processes that cause MHWs are considered with respect to their possible predictability. Specifically, MHW predictability is considered on temporal scales ranging from short-term weather (atmospheric blocking and oceanic eddies), to multiyear-to-decadal (via oceanic Rossby wave teleconnections), and centennial (climate change) time scales. Modes of climate variability, in particular ENSO, play an important role in modulating MHW likelihoods around the world (Scannell *et al.* 2016; Oliver *et al.* 2018*a*; Holbrook *et al.* 2019) with impacts on marine ecosystems (Holbrook *et al.* 2020*a*). The importance of ocean mixed layer depths and heat content (e.g. Behrens *et al.* 2019) have been explored as mechanisms to precondition MHW likelihood (Holbrook *et al.* 2020*b*). Holbrook *et al.* (2020*b*) further argued that event-based monitoring and skilful MHW prediction have the potential to provide critical information and guidance for marine conservation, fisheries, and aquaculture management.

A better understanding of the relevant time scales and drivers of SST variability will be beneficial to inform the potential predictability of SST and extremes. Some preliminary analysis, based on outputs from the Commonwealth Scientific and Industrial Research Organisation's (CSIRO) Climate Analysis Forecast Ensemble (CAFE) System (O'Kane *et al.* 2019) indicated that multi-year forecast skill of MHWs in specific regions around Australia may be possible (Cougnon *et al.* 2018). Another study found significant correlations between a range of modes of climate variability and remote MHWs (Holbrook *et al.* 2019). These are some examples of studies looking into the drivers and predictors of MHWs, but there is also active work on MHW prediction. A collaboration between CSIRO and the Australian Bureau of Meteorology is developing experimental seasonal MHW forecast products for Australia's marine region (https://research.csiro.au/mri-research-portfolio/home/climate-impacts-adaptation/marine-heatwaves/dynamical-forecasting-of-marine-heatwaves/) using the ACCESS-S seasonal prediction model (Hudson *et al.* 2017).

With regards to the case study regions analysed in Section 4, there are varying levels of predictability discussed in the literature. Along the Western Australian coast, for example, there appears to be a link between the occurrence of the strongest MHWs in the region and La Niña (Feng *et al.* 2013; Benthuysen *et al.* 2014; Kataoka *et al.* 2014, 2017; Marshall *et al.* 2015; Zinke *et al.* 2015). Holbrook *et al.* (2019) showed that there is a significant correlation between MHWs in the Western Australian region and ENSO, with >50% more MHW days occurring during La Niña, as compared to El Niño.

Elevated SSTs and coral bleaching in the GBR can be related to ENSO-related events (e.g. 1998 and 2016) as well as regional weather conditions (2002, 2006, and 2017) such as increased solar radiation, low cloud cover, reduced wind (decreases mixing and affects air-sea fluxes), and reduced rainfall (Smith and Spillman 2019). El Niño-related coral bleaching in the GBR is associated with anomalously warm ocean waters due to reduced cloud cover from a weakened monsoon that enhances radiative heating, and an enhanced South Equatorial Current flowing into the Coral Sea (Smith and Spillman 2019). Therefore, there is potential predictability at two spatial and temporal scales (those related to ENSO and those to regional weather patterns), with associated differences in the forecast lead times.

For the Tasman Sea, about half of the historical occurrences of MHWs in the region were primarily due to increased EAC Extension poleward transport of warm water (Li *et al.* 2020). Slowly propagating oceanic Rossby waves, generated by wind stresses in the interior South Pacific and restored at the planetary scale, appear to be an important mechanism for modulating the intensity of the EAC Extension. Importantly, 2–3 years before the Rossby waves cause the EAC Extension to intensify, their impact can already be seen in changes in sea surface heights around New Zealand (Li *et al.* 2020). The slow propagation speeds of Rossby waves supports the possibility that the increased likelihoods of MHWs that impact southeast Australia may be forecast years in advance, with important implications for fisheries and the environment in this region.

Recently there has been increasing interest in utilising machine learning approaches for predicting SST extremes and MHWs at time scales ranging from seasonal to climate (e.g. Yang *et al.* 2018; Ham *et al.* 2019; Boschetti *et al.* 2021). Typically, machine learning approaches synthesise datasets and can then provide sequential time series forecasting. For example, neural networks can be trained to

learn seasonal patterns in SST, and then identify the preconditional features for predicting extreme events (Yang *et al.* 2018; Holbrook *et al.* 2020*b*).

6 Discussion and conclusions

This paper has provided a historical analysis, review and catalogue of detected MHWs from SST observations around Australia since 1982. Our results and data outputs are based on analysis and application of the Hobday *et al.* (2016, 2018) MHW definition and categorisation to interpolated daily SST observations over the recent satellite era, and includes mean metrics, trends, and classifications. The longest duration and strongest intensity MHWs were also identified in selected case-study regions: Western Australia, Torres Strait, GBR, Tasman Sea, and the South Australian Basin. The study provides a catalogue of MHWs, primarily in a statistical sense. Some details of associated impacts identified in the literature have also been provided. There is an emerging body of work on the potential predictability of MHWs, some of which was briefly reviewed herein, with a focus on the Australian region.

Interpretation of some MHW metrics needs to be treated with caution. For example, trends in MHW metrics can be difficult to compute, due to data sparsity, i.e. MHWs do not necessarily occur in each year, and in particular, long periods without a MHW can bias trend calculations. These metrics for a broad area, such as the Australia-wide analysis (Fig. 1*d–i*), can give some indication of changes, but are less informative for smaller regions and especially near coastlines (Marin *et al.* 2021). Thus, the equivalent timeseries of metrics (i.e. Fig. 1*g–i*) were not presented for the case study regions. Conversely, it must be acknowledged that averaging across a very broad area can dilute more localised extreme events. Nevertheless, annual counts of MHW days (as in panel *a* of Figs 5–9) give a sense of MHW trends in each of the regions which may act to reduce the magnitude of some of these extremes if they were analysed and presented in smaller subregions.

Another consideration is the choice of climatological baseline period, which in this study was 1983–2012 following the recommendation of Hobday *et al.* (2018). Different baseline periods may not qualitatively affect MHW detection, but they will result in quantitively different MHW metrics. Using a more recent baseline (i.e. shifted closer to the present day), for example, will tend to weaken computed MHW intensities and shorten their duration, since more recent periods tend to be warmer due to climate change (Schlegel *et al.* 2019). However this is not a strict rule, as decadal and multidecadal variations can also shift the climatology. A fixed reference climatology is generally favoured in impact studies, because changes in extremes are measured relative to this 'normal' level. But fixing the baseline does not account for adaptative and evolutionary capacities. The recently developed 'thermal displacement' view of MHWs largely avoids complications of baseline choice, since MHWs are characterised by spatial shifts of surface temperature contours, rather than by local temperature anomalies (Jacox *et al.* 2020).

The MHW metrics presented in this study are not exhaustive. Other potentially informative metrics include degree heating weeks, which is a measure of cumulative intensity typically used to understand coral bleaching risks (e.g. Eakin *et al.* 2010), and return intervals. For brevity, and to retain a focus on primary metrics of MHWs, these quantities were not analysed here, but they may be useful for the analysis of the ecological impacts of MHWs.

An important finding of this study is that many regions around Australia have yet to experience Strong or Extreme category MHWs. In particular, the GBR has yet to experience a large-scale Severe (Category 3) MHW, despite widespread ecological damage, including high levels of coral bleaching, from elevated ocean temperatures in recent years. An Extreme (Category 4) MHW in the GBR during the summer months would be expected to result in extensive devastation. Understanding why some regions have experienced quite different maximum categories is important for impact-related studies, and the spatial maps presented herein provide a starting point for such possible future research avenues.

References

Abdo DA, Bellchambers LM, Evans SN (2012) Turning up the heat: increasing temperature and coral bleaching at the high latitude coral reefs of the Houtman Abrolhos islands. *PLoS One* **7**, e43878. doi:10.1371/journal.pone.0043878

Arias-Ortiz A, Serrano O, Masqué P, Lavery PS, Mueller U, Kendrick GA, Rozaimi M, Esteban A, Fourqurean JW, Marbà N, Mateo MA, Murray K, Rule MJ, Duarte CM (2018) A marine heatwave drives massive losses from the world's largest seagrass carbon stocks. *Nature Climate Change* **8**, 338–344. doi:10.1038/s41558-018-0096-y

Banzon V, Smith TM, Steele M, Huang B, Zhang HM (2020) Improved estimation of proxy sea surface temperature in the arctic. *Journal of Atmospheric and Oceanic Technology* **37**, 341–349. doi:10.1175/JTECH-D-19-0177.1

Behrens E, Fernandez D, Sutton P (2019) Meridional oceanic heat transport influences marine heatwaves in the Tasman Sea on interannual to decadal timescales. *Frontiers in Marine Science* **6**, 228. doi:10.3389/fmars.2019.00228

Benthuysen JA, Feng M, Zhong L (2014) Spatial patterns of warming off Western Australia during the 2011 Ningaloo Niño: quantifying impacts of remote and local forcing. *Continental Shelf Research* **91**, 232–246. doi:10.1016/j.csr.2014.09.014

Benthuysen JA, Oliver ECJ, Feng M, Marshall AG (2018) Extreme Marine warming across tropical Australia during austral summer 2015–2016. *Journal of Geophysical Research: Oceans* **123**, 1301–1326. doi:10.1002/2017JC013326

Berkelmans R, Oliver JK (1999) Large-scale bleaching of corals on the Great Barrier Reef. *Coral Reefs* **18**, 55–60. doi:10.1002/ecy.2092

Berkelmans R, Weeks SJ, Steinberga CR (2010) Upwelling linked to warm summers and bleaching on the Great Barrier Reef. *Limnology and Oceanography* **55**, 2634–2644. doi:10.4319/lo.2010.55.6.2634

Bond NA, Cronin MF, Freeland H, Mantua N (2015) Causes and impacts of the 2014 warm anomaly in the NE Pacific. *Geophysical Research Letters* **42**, 3414–3420. doi:10.1002/2015GL063306

Boschetti F, Feng M, Zhang X, Hartog JR, Hobday AJ (2021) Statistical prediction of marine heatwaves via machine learning. Conference Presentation at Australian Meteorological and Oceanographic

Society Online Conference, 8–12 February 2021. Abstracts available at https://amos.eventsair.com/amos-2021/abstract-book
Bureau of Meteorology (2020) 2020 marine heatwave on the Great Barrier Reef. Available at http://www.bom.gov.au/environment/doc/marine-heatwave-2016.pdf
Caputi N, Kangas M, Denham A, Feng M, Pearce A, Hetzel Y, Chandrapavan A (2016) Management adaptation of invertebrate fisheries to an extreme marine heat wave event at a global warming hot spot. *Ecology and Evolution* **6**, 3583–3593. doi:10.1002/ece3.2137
Caputi N, Kangas M, Chandrapavan A, Hart A, Feng M, Marin M, de Lestang S (2019) Factors affecting the recovery of Invertebrate stocks from the 2011 Western Australian extreme marine heatwave. *Frontiers in Marine Science* **6**, 484. doi:10.3389/fmars.2019.00484
Cavole LM, Demko AM, Diner RE, Giddings A, Koester I, Pagniello CMLS, Paulsen ML, Ramirez-Valdez A, Schwenck SM, Yen NK, Zill ME, Franks PJS (2016) Biological impacts of the 2013–2015 warm-water anomaly in the northeast Pacific: winners, losers, and the future. *Oceanography* **29**, 273–285. doi:10.5670/oceanog.2016.32
Cougnon EA, Holbrook NJ, O'Kane TJ, Oliver ECJ, Bindoff NL (2018) Representation of ocean temperature extremes in the ACCESS Decadal Prediction System Climate Analysis Forecast Ensemble. NESP ESCC Project 2.3 (component 2) Metadata Report #2. Australia.
Di Lorenzo E, Mantua N (2016) Multi-year persistence of the 2014/15 North Pacific marine heatwave. *Nature Climate Change* **6**, 1042–1047. doi:10.1038/nclimate3082
Duke NC, Kovacs JM, Griffiths AD, Preece L, Hill DJE, van Oosterzee P, Mackenzie J, Morning HS, Burrows D (2017) Large-scale dieback of mangroves in Australia. *Marine and Freshwater Research* **68**, 1816–1829. doi:10.1071/mf16322
Duran ER, England MH, Spence P (2020) Surface ocean warming around Australia driven by interannual variability and long-term trends in Southern Hemisphere westerlies. *Geophysical Research Letters* **47**, e2019GL086605. doi:10.1029/2019GL086605
Eakin CM, Morgan JA, Heron SF, Smith TB, Liu G, Alvarez-Filip L, Baca B, Bartels E, Bastidas C, Bouchon C (2010) Caribbean corals in crisis: record thermal stress, bleaching, and mortality in 2005. *PLoS One* **5**, e13969. doi:10.1371/journal.pone.0013969
Feng M, McPhaden MJ, Xie SP, Hafner J (2013) La Niña forces unprecedented leeuwin current warming in 2011. *Scientific Reports* **3**, 1277. doi:10.1038/srep01277
Feng M, Hendon HH, Xie SP, Marshall AG, Schiller A, Kosaka Y, Caputi N, Pearce A (2015) Decadal increase in Ningaloo Niño since the late 1990s. *Geophysical Research Letters* **42**, 104–112. doi:10.1002/2014GL062509
Feng M, Caputi N, Chandrapavan A, Chen M, Hart A, Kangas M (2021) Multi-year marine cold-spells off the west coast of Australia and effects on fisheries. *Journal of Marine Systems* **214**, 103473. doi:10.1016/j.jmarsys.2020.103473
Frölicher TL, Fischer EM, Gruber N (2018) Marine heatwaves under global warming. *Nature* **560**, 360–364. doi:10.1038/s41586-018-0383-9
GBRMPA (2004) Great Barrier Reef marine park zoning plan 2003. Great Barrier Reef Marine Park Authority, Queensland, Australia.
GBRMPA (2014) Great Barrier Reef outlook report 2014. Townsville, Queensland, Australia.
GBRMPA (2016) Interim report: 2016 coral bleaching event on the Great Barrier Reef. Townsville, Australia. Available at http://hdl.handle.net/11017/3044
GBRMPA (2017) Final report: 2016 coral bleaching event on the Great Barrier Reef. Townsville, Australia.
Ham Y-G, Kim J-H, Luo J (2019) Deep learning for multi-year ENSO forecasts. *Nature* **573**, 568–572. doi:10.1038/s41586-019-1559-7
Harris T, Hope P, Oliver ECJ, Smalley R, Arblaster JM, Holbrook N, Duke N, Pearce K, Braganza K, Bindoff N (2017) Climate drivers of the 2015 Gulf of Carpentaria mangrove dieback, Earth Systems and Climate Change Hub Technical Report No. 1. Australia.
Hobday AJ, Pecl GT (2014) Identification of global marine hotspots: sentinels for change and vanguards for adaptation action. *Reviews in Fish Biology and Fisheries* **24**, 415–425. doi:10.1007/s11160-013-9326-6
Hobday AJ, Alexander LV, Perkins-Kirkpatrick SE, Smale DA, Straub SC, Oliver ECJ, Benthuysen JA, Burrows MT, Donat MG, Feng M, Holbrook NJ, Moore PJ, Scannell HA, Sen Gupta A, Wernberg T (2016) A hierarchical approach to defining marine heatwaves. *Progress in Oceanography* **141**, 227–238. doi:10.1016/j.pocean.2015.12.014
Hobday AJ, Oliver ECJ, Sen Gupta A, Benthuysen JA, Burrows MT, Donat MG, Holbrook NJ, Moore PJ, Thomsen MS, Wernberg T, Smale DA (2018) Categorizing and naming marine heatwaves. *Oceanography* **31**, 162–173. doi:10.5670/oceanog.2018.205
Holbrook NJ, Bindoff NL (1997) Interannual and decadal temperature variability in the southwest Pacific Ocean between 1955 and 1988. *Journal of Climate* **10**, 1035–1049. doi:10.1175/1520-0442(1997)010<1035:IADTVI>2.0.CO;2
Holbrook NJ, Scannell HA, Sen Gupta A, Benthuysen JA, Feng M, Oliver ECJ, Alexander LV, Burrows MT, Donat MG, Hobday AJ, Moore PJ, Perkins-Kirkpatrick SE, Smale DA, Straub SC, Wernberg T (2019) A global assessment of marine heatwaves and their drivers. *Nature Communications* **10**, 2624. doi:10.1038/s41467-019-10206-z
Holbrook NJ, Claar DC, Hobday AJ, McInnes K, Oliver ECJ, Sen Gupta A, Widlansky MJ, Zhang X (2020*a*) ENSO-driven ocean extremes and their ecosystem impacts. In 'El Niño Southern oscillation in a changing climate'. (Eds MJ McPhaden, A Santoso, W Cai) pp. 409–428. (American Geophysical Union (AGU): Washington, DC)
Holbrook NJ, Sen Gupta A, Oliver ECJ, Hobday AJ, Benthuysen JA, Scannell HA, Smale DA, Wernberg T (2020*b*). Keeping pace with marine heatwaves. *Nature Reviews Earth & Environment* **1**, 482–493. doi:10.1038/s43017-020-0068-4
Huang B, Liu C, Banzon V, Freeman E, Graham G, Hankins B, Smith T, Zhang H-M (2021*a*). Improvements of the daily optimum sea surface temperature (DOISST) - version 2.1. *Journal of Climate* **34**, 2923–2939.
Huang B, Liu C, Freeman E, Graham G, Smith T, Zhang HM (2021*b*). Assessment and intercomparison of NOAA daily optimum interpolation sea surface temperature (DOISST) version 2.1. *Journal of Climate* **34**, 7421–7441. doi:10.1175/JCLI-D-20-0166.1
Hudson D, Alves O, Hendon HH, Lim E-P, Liu G, Luo J-J, MacLachlan C, Marshall AG, Shi L, Wang G, Wedd R, Young G, Zhao M, Zhou X (2017) ACCESS-S1: the new Bureau of Meteorology multi-week to seasonal prediction system. *Journal of Southern Hemisphere Earth Systems Science* **67**, 132–159. doi:10.22499/3.6703.001
Hughes TP, Kerry JT, Álvarez-Noriega M, Álvarez-Romero JG, Anderson KD, Baird AH, Babcock RC, Beger M, Bellwood DR, Berkelmans R, Bridge TC, Butler IR, Byrne M, Cantin NE, Comeau S, Connolly SR, Cumming GS, Dalton SJ, Diaz-Pulido G, Eakin CM, Figueira WF, Gilmour JP, Harrison HB, Heron SF, Hoey AS, Hobbs JPA, Hoogenboom MO, Kennedy EV, Kuo CY, Lough JM, Lowe RJ, Liu G, McCulloch MT, Malcolm HA, McWilliam MJ, Pandolfi JM, Pears RJ, Pratchett MS, Schoepf V, Simpson T, Skirving WJ, Sommer B, Torda G, Wachenfeld DR, Willis BL, Wilson SK (2017) Global warming and recurrent mass bleaching of corals. *Nature* **543**, 373–377. doi:10.1038/nature21707
Hughes TP, Kerry JT, Baird AH, Connolly SR, Chase TJ, Dietzel A, Hill T, Hoey AS, Hoogenboom MO, Jacobson M, Kerswell A, Madin JS, Mieog A, Paley AS, Pratchett MS, Torda G, Woods RM (2019) Global warming impairs stock–recruitment dynamics of corals. *Nature* **568**, 387–390. doi:10.1038/s41586-019-1081-y
Jacox MG, Alexander MA, Bograd SJ, Scott JD (2020) Thermal displacement by marine heatwaves. *Nature* **584**, 82–86. doi:10.1038/s41586-020-2534-z
Johnson JE, Bertram I, Chin A, Moore BR, Pratchett M, Welch DJ, Williams A, Bell JD, Govan H (2018) Impacts of climate change on fish and shellfish relevant to the Pacific Islands. Pacific Marine Climate Change Report Card: Science Review.
Johnson JE, Allain V, Basel B, Bell JD, Chin A, Dutra LXC, Hooper E, Loubser D, Lough J, Moore BR, *et al.* (2020) Impacts of climate change on Marine resources in the Pacific Island Region. In 'Climate Change and Impacts in the Pacific'. pp. 359–402. (Springer)
Kataoka T, Tozuka T, Behera SK, Yamagata T (2014) On the Ningaloo Niño/Niña. *Climate Dynamics* **43**, 1463–1482. doi:10.1007/s00382-013-1961-z
Kataoka T, Tozuka T, Yamagata T (2017) Generation and decay mechanisms of Ningaloo Niño/Niña. *Journal of Geophysical Research: Oceans* **122**, 8913–8932. doi:10.1002/2017JC012966

Laufkötter C, Zscheischler J, Frölicher TL (2020) High-impact marine heatwaves attributable to human-induced global warming. *Science* **369**, 1621–1625. doi:10.1126/science.aba0690

Li Z, Holbrook NJ, Zhang X, Oliver ECJ, Cougnon EA (2020) Remote forcing of Tasman Sea marine heatwaves. *Journal of Climate* **33**, 5337–5354. doi:10.1175/JCLI-D-19-0641.1

Llewellyn LE (2010) Revisiting the association between sea surface temperature and the epidemiology of fish poisoning in the South Pacific: Reassessing the link between ciguatera and climate change. *Toxicon* **56**, 691–697. doi:10.1016/j.toxicon.2009.08.011

Marin M, Feng M, Phillips HE, Bindoff NL (2021) A global, multiproduct analysis of coastal marine heatwaves: distribution, characteristics and long-term trends. *Journal of Geophysical Research: Oceans* **126**, e2020JC016708. doi:10.1029/2020jc016708

Marshall AG, Hendon HH, Feng M, Schiller A (2015) Initiation and amplification of the Ningaloo Niño. *Climate Dynamics* **45**, 2367–2385. doi:10.1007/s00382-015-2477-5

McInnes KL, Kajtar JB, Holbrook NJ, Hemer M, Hernaman V (2021) Coastal climate services: a review of needs for coastal, marine and offshore applications. Earth Systems and Climate Change Hub Report No. 18. Australia.

McPhaden MJ (1999) Genesis and evolution of the 1997–98 El Niño. *Science* **283**, 950–955. doi:10.1126/science.283.5404.950

Mills KE, Pershing AJ, Brown CJ, Chen Y, Chiang FS, Holland DS, Lehuta S, Nye JA, Sun JC, Thomas AC, Wahle RA (2013) Fisheries management in a changing climate: Lessons from the 2012 ocean heat wave in the Northwest Atlantic. *Oceanography* **26**, 191–195. doi:10.5670/oceanog.2013.27

Misra R, Sérazin G, Meissner KJ, Sen Gupta A (2021) Projected changes to Australian Marine Heatwaves. *Geophysical Research Letters* **48**, e2020GL091323. doi:10.1029/2020GL091323

Moore JAY, Bellchambers LM, Depczynski MR, Evans RD, Evans SN, Field SN, Friedman KJ, Gilmour JP, Holmes TH, Middlebrook R, Radford BT, Ridgway T, Shedrawi G, Taylor H, Thomson DP, Wilson SK (2012) Unprecedented mass bleaching and loss of coral across 12° of latitude in Western Australia in 2010-11. *PLoS One* **7**, e51807. doi:10.1371/journal.pone.0051807

NESP Earth Systems and Climate Change Hub (2018*a*) Climate change and the Shark Bay World Heritage Area: foundations for a climate change adaptation strategy and action plan. Earth Systems and Climate Change Hub Report No. 7. Australia.

NESP Earth Systems and Climate Change Hub (2018*b*) Climate change in the Torres Strait: implications for fisheries and marine ecosystems. Australia.

NTSC (2016) September mud crabs in focus. Darwin, Australia. doi:10.32964/tj15.9

O'Kane TJ, Sandery PA, Monselesan DP, Sakov P, Chamberlain MA, Matear RJ, Collier MA, Squire DT, Stevens L (2019) Coupled data assimilation and ensemble initialization with application to multiyear ENSO prediction. *Journal of Climate* **32**, 997–1024. doi:10.1175/jcli-d-18-0189.1

Oliver ECJ (2019) Mean warming not variability drives marine heatwave trends. *Climate Dynamics* **53**, 1653–1659. doi:10.1007/s00382-019-04707-2

Oliver ECJ, Holbrook NJ (2018) Variability and long-term trends in the shelf circulation off Eastern Tasmania. *Journal of Geophysical Research: Oceans* **123**, 7366–7381. doi:10.1029/2018JC013994

Oliver ECJ, Benthuysen JA, Bindoff NL, Hobday AJ, Holbrook NJ, Mundy CN, Perkins-Kirkpatrick SE (2017) The unprecedented 2015/16 Tasman Sea marine heatwave. *Nature Communications* **8**, 1038. doi:10.1038/ncomms16101

Oliver ECJ, Donat MG, Burrows MT, Moore PJ, Smale DA, Alexander LV, Benthuysen JA, Feng M, Sen Gupta A, Hobday AJ, Holbrook NJ, Perkins-Kirkpatrick SE, Scannell HA, Straub SC, Wernberg T (2018*a*). Longer and more frequent marine heatwaves over the past century. *Nature Communications* **9**, 1324. doi:10.1038/s41467-018-03732-9

Oliver ECJ, Perkins-Kirkpatrick SE, Holbrook NJ, Bindoff NL (2018*b*). Anthropogenic and natural influences on record 2016 marine heat waves. *Bulletin of the American Meteorological Society* **99**, S44–S48. doi:10.1175/bams-d-17-0093.1

Oliver ECJ, Burrows MT, Donat MG, Sen Gupta A, Alexander LV, Perkins-kirkpatrick SE, Benthuysen JA, Hobday AJ, Holbrook NJ, Moore PJ, Thomsen MS, Wernberg T, Smale DA (2019) Projected marine heatwaves in the 21st century and the potential for ecological impact. *Frontiers in Marine Science* **6**, 734. doi:10.3389/fmars.2019.00734

Pearce AF, Feng M (2013) The rise and fall of the "marine heat wave" off Western Australia during the summer of 2010/2011. *Journal of Marine Systems* **111–112**, 139–156. doi:10.1016/j.jmarsys.2012.10.009

Perkins-Kirkpatrick SE, King AD, Cougnon EA, Grose MR, Oliver ECJ, Holbrook NJ, Lewis SC, Pourasghar F (2019) The role of natural variability and anthropogenic climate change in the 2017/18 Tasman Sea marine heatwave. *Bulletin of the American Meteorological Society* **100**, S105–S110. doi:10.1175/BAMS-D-18-0116.1

Rayner N, Tsushima Y, Atkinson C, Good S, Roberts M, Martin G, Ackerley D, Titchner H, Mao C, Xavier P, Comer R, Hu Y, Beggs H, Wang XH, Margaritis G, Renshaw R, Lamas L, Esteves R, Almeida S, de Azevedo E, Correia C, Reis F, Willén U (2019) SST-CCI-Phase-II SST CCI climate assessment report. Available at https://climate.esa.int/documents/268/SST_cci_CAR_v1.pdf

Reynolds RW, Smith TM, Liu C, Chelton DB, Casey KS, Schlax MG (2007) Daily high-resolution-blended analyses for sea surface temperature. *Journal of Climate* **20**, 5473–5496. doi:10.1175/2007JCLI1824.1

Ridgway KR (1997) Seasonal cycle of the East Australian current. *Journal of Geophysical Research: Oceans* **102**, 22921–22936. doi:10.1029/97JC00227

Ridgway KR (2007) Long-term trend and decadal variability of the southward penetration of the East Australian Current. *Geophysical Research Letters* **34**, L13613. doi:10.1029/2007GL030393

Roberts SD, van Ruth P, Wilkinson C, Bastianello SB, Bansemer MS (2019) Marine heatwave, harmful algae blooms and an extensive fish kill event during 2013 in South Australia. *Frontiers in Marine Science* **6**, 610. doi:10.3389/fmars.2019.00610

Scannell H, Pershing A, Alexander MA, Thomas AC, Mills KE (2016) Frequency of marine heatwaves in the North Atlantic and North Pacific since 1950. *Geophysical Research Letters* **43**, 2069–2076. doi:10.1002/2015GL067308.Received

Schiller A, Ridgway KR, Steinberg CR, Oke PR (2009) Dynamics of three anomalous SST events in the Coral Sea. *Geophysical Research Letters* **36**, L06606. doi:10.1029/2008GL036997

Schlegel RW, Oliver ECJ, Hobday AJ, Smit AJ (2019) Detecting marine heatwaves with sub-optimal data. *Frontiers in Marine Science* **6**, 737. doi:10.3389/fmars.2019.00737

Sen Gupta A, Thomsen M, Benthuysen JA, Hobday AJ, Oliver ECJ, Alexander LV, Burrows MT, Donat MG, Feng M, Holbrook NJ, Perkins-Kirkpatrick S, Moore PJ, Rodrigues RR, Scannell HA, Taschetto AS, Ummenhofer CC, Wernberg T, Smale DA (2020) Drivers and impacts of the most extreme marine heatwaves events. *Scientific Reports* **10**, 19359. doi:10.1038/s41598-020-75445-3

Skinner MP, Brewer TD, Johnstone R, Fleming LE, Lewis RJ (2011) Ciguatera fish poisoning in the Pacific Islands (1998 to 2008). *PLOS Neglected Tropical Diseases* **5**, e1416. doi:10.1371/journal.pntd.0001416

Smale DA, Wernberg T (2013) Extreme climatic event drives range contraction of a habitat-forming species. *Proceedings of the Royal Society B: Biological Sciences* **280**, 20122829. doi:10.1098/rspb.2012.2829

Smale DA, Wernberg T, Oliver ECJ, Thomsen MS, Harvey BP, Straub SC, Burrows MT, Alexander LV, Benthuysen JA, Donat MG, Feng M, Hobday AJ, Holbrook NJ, Perkins-Kirkpatrick SE, Scannell HA, Sen Gupta A, Payne BL, Moore PJ (2019) Marine heatwaves threaten global biodiversity and the provision of ecosystem services. *Nature Climate Change* **9**, 306–312. doi:10.1038/s41558-019-0412-1

Smith G, Spillman C (2019) New high-resolution sea surface temperature forecasts for coral reef management on the Great Barrier Reef. *Coral Reefs* **38**, 1039–1056. doi:10.1007/s00338-019-01829-1

Thomsen MS, Mondardini L, Alestra T, Gerrity S, Tait L, South PM, Lilley SA, Schiel DR (2019) Local extinction of bull kelp (*Durvillaea* spp.) due to a marine heatwave. *Frontiers in Marine Science* **6**, 84. doi:10.3389/fmars.2019.00084

Thomson JA, Burkholder DA, Heithaus MR, Fourqurean JW, Fraser MW, Statton J, Kendrick GA (2015) Extreme temperatures, foundation species, and abrupt ecosystem change: an example from an

iconic seagrass ecosystem. *Global Change Biology* **21**, 1463–1474. doi:10.1111/gcb.12694

Ugalde SC, Preston J, Ogier E, Crawford C (2018) Analysis of farm management strategies following herpesvirus (OsHV-1) disease outbreaks in Pacific oysters in Tasmania, Australia. *Aquaculture* **495**, 179–186. doi:10.1016/j.aquaculture.2018.05.019

Wernberg T, Smale DA, Tuya F, Thomsen MS, Langlois TJ, de Bettignies T, Bennett S, Rousseaux CS (2013) An extreme climatic event alters marine ecosystem structure in a global biodiversity hotspot. *Nature Climate Change* **3**, 78–82. doi:10.1038/nclimate1627

Wernberg T, Bennett S, Babcock RC, De Bettignies T, Cure K, Depczynski M, Dufois F, Fromont J, Fulton CJ, Hovey RK, Harvey, ES, Holmes TH, Kendrick GA, Radford B, Santana-Garcon J, Saunders BJ, Smale DA, Thomsen MS, Tuckett CA, Tuya F, Vanderklift MA, Wilson S (2016) Climate-driven regime shift of a temperate marine ecosystem. *Science* **353**, 169–172. doi:10.1126/science.aad8745

Wild K (2016) Indigenous rangers on the frontline of coral bleaching in remote Australia. Available at http://www.abc.net.au/news/2016-07-11/indigenous-rangers-on-the-frontline-of-coral-bleaching/7557646

Wu L, Cai W, Zhang L, Nakamura H, Timmermann A, Joyce T, McPhaden MJ, Alexander MA, Qiu B, Visbeck M, Chang P, Giese B (2012) Enhanced warming over the global subtropical western boundary currents. *Nature Climate Change* **2**, 161–166. doi:10.1038/nclimate1353

Yang Y, Dong J, Sun X, Lima E, Mu Q, Wang X (2018) A CFCC-LSTM model for sea surface temperature prediction. *IEEE Geoscience and Remote Sensing Letters* **15**, 207–211. doi:10.1109/LGRS.2017.2780843

Yang C, Leonelli FE, Marullo S, Artale V, Beggs H, Nardelli BB, Chin TM, De Toma V, Good S, Huang B, Merchant CJ, Sakurai T, Santoleri R, Vazquez-Cuervo J, Zhang HM, Pisano A (2021) Sea surface temperature intercomparison in the framework of the copernicus climate change service (C3S). *Journal of Climate* **34**, 5257–5283. doi:10.1175/JCLI-D-20-0793.1

Zhang L, Han W, Li Y, Shinoda T (2018) Mechanisms for generation and development of the Ningaloo Niño. *Journal of Climate* **31**, 9239–9259. doi:10.1175/JCLI-D-18-0175.1

Zinke J, Hoell A, Lough JM, Feng M, Kuret AJ, Clarke H, Ricca V, Rankenburg K, McCulloch MT (2015) Coral record of southeast Indian Ocean marine heatwaves with intensified Western Pacific temperature gradient. *Nature Communications* **6**, 8562. doi:10.1038/ncomms9562

Data availability. The NOAA 0.25-degree Daily Optimum Interpolation Sea Surface Temperature (DOISST), Version 2.1 description and metadata are available at https://doi.org/10.25921/RE9P-PT57, and annual datafiles are provided courtesy of NOAA/OAR/ESRL PSL at https://psl.noaa.gov/data/gridded/data.noaa.oisst.v2.highres.html. The observed Oceanic Niño Index was provided by the NOAA Climate Prediction Center, and is available from https://psl.noaa.gov/data/correlation/oni.data. The marine heatwave metrics generated by this study, along with the code, are available for download at https://github.com/jbkajtar/mhw_australia.

Conflicts of interest. Neil Holbrook is an Associate Editor of the Journal of Southern Hemisphere Earth Systems Science but was blinded from the peer-review process for this paper.

Declaration of funding. This study was completed under funding received from the Australian Government's National Environmental Science Program (NESP) Earth Systems and Climate Change (ESCC) Hub, and the NESP Phase 2 Climate Systems Hub. NJH and JBK were supported by the Australian Research Council's Centre of Excellence for Climate Extremes (CE170100023).

Acknowledgements. We acknowledge support from the Australian Government's National Environmental Science Program (NESP) Earth Systems and Climate Change (ESCC) Hub, and the Australian Research Council's Centre of Excellence for Climate Extremes. The research was conducted under ESCC Hub Project 5.8: 'Marine and coastal climate services for extremes'. We acknowledge the input and support of project leader Kathleen L. McInnes and the whole Project 5.8 team. JBK and NJH acknowledge further support from the NESP Phase 2 Climate Systems Hub. We thank the National Oceanic and Atmospheric Administration (NOAA) for making available the DOISST and Oceanic Niño Index datasets. The National Computational Infrastructure (NCI), which is supported by the Australian Government, was utilised for processing and analysing the data. We thank Eric C. J. Oliver for his marine heatwave detection code, which is publicly available at https://github.com/ecjoliver/marineHeatWaves. The authors wish to thank the two anonymous reviewers and the editors at JSHESS for taking the time to review our manuscript. Their careful consideration and suggestions helped to substantially improve the presentation of this study.

Author affiliations

[A]Institute for Marine and Antarctic Studies, University of Tasmania, Hobart, Tas., Australia.

[B]Australian Research Council Centre of Excellence for Climate Extremes, University of Tasmania, Hobart, Tas., Australia.

[C]Climate Science Centre, CSIRO Oceans and Atmosphere, Aspendale, Vic., Australia.